

Safe targeting of T cell acute lymphoblastic leukemia by pathology-specific NOTCH inhibition

Roger A. Habets^{1,2#}, Charles E. de Bock^{3,4,5#}, Lutgarde Serneels^{1,2}, Inge Lodewijkx^{3,4}, Delphine Verbeke^{3,4}, David Nittner^{6,7}, Rajeshwar Narlawar^{1,2}, Sofie Demeyer^{3,4}, James Dooley^{2,8}, Adrian Liston^{2,8}, Tom Taghon^{9,10}, Jan Cools^{3,4,*} and Bart de Strooper^{1,2,11,*}

¹ Department of Neurosciences, Leuven Institute for Neuroscience and Disease, (LIND), KU Leuven, 3000 Leuven, Belgium

² VIB Center for Brain and Disease Research, VIB, 3000 Leuven, Belgium

³ Center for Human Genetics, KU Leuven, 3000 Leuven, Belgium

⁴ VIB Center for Cancer Biology, VIB, 3000 Leuven, Belgium

⁵ Children's Cancer Institute, Lowy Cancer Research Centre, UNSW, Sydney, NSW 2052, Australia

⁶ Histopathology Expertise Center, VIB-KU Leuven Center for Cancer Biology, 3000 Leuven, Belgium

⁷ Department of Oncology, KU Leuven, 3000 Leuven, Belgium

⁸ Department of Microbiology and Immunology, KU Leuven, 3000 Leuven, Belgium

⁹ Department of Diagnostic Sciences, Faculty of Medicine and Health Sciences, Ghent University, Ghent 9000, Belgium

¹⁰ Cancer Research Institute Ghent, 9000 Ghent, Belgium

¹¹ Dementia Research Institute, University College London, London WC1E 6BT, UK

These authors contributed equally to this work

* **Corresponding authors:** bart.destrooper@kuleuven.vib.be or jan.cools@kuleuven.vib.be

Abstract

Given the high frequency of activating *NOTCH1* mutations in T cell acute lymphoblastic leukemia (T-ALL), inhibition of the γ -secretase complex remains an attractive target to prevent ligand-independent release of the cytoplasmic tail and oncogenic NOTCH1 signaling. However, four different γ -secretase complexes exist, and available inhibitors block all complexes equally. As a result, these cause severe “on-target” gastrointestinal tract, skin, and thymus toxicity, limiting their therapeutic application. Here, we demonstrate that genetic deletion or pharmacologic inhibition of the Presenilin-1 (PSEN1) subclass of γ -secretase complexes is highly effective in decreasing leukemia whilst avoiding dose-limiting toxicities. Clinically, T-ALL samples were found to selectively express only PSEN1-containing γ -secretase complexes. The conditional knock-out of *Psen1* in developing T cells attenuated the development of a mutant NOTCH1-driven leukemia in mice in vivo but did not abrogate normal T cell development. Treatment of T-ALL cell lines with the selective PSEN1 inhibitor MRK-560 effectively decreased mutant NOTCH1 processing and led to cell cycle arrest. These observations were extended to T-ALL patient-derived xenografts in vivo, demonstrating that MRK-560 treatment decreases leukemia burden and increased overall survival without any associated gut toxicity. Therefore, PSEN1-selective compounds provide a potential therapeutic strategy for safe and effective targeting of T-ALL and possibly also for other diseases in which NOTCH signaling plays a role.

One Sentence Summary

Selective inhibition of γ -secretase complexes targets T-ALL without the dose-limiting side effects of complete γ -secretase inhibition.

Introduction

γ -Secretases are a group of widely expressed intramembrane-cleaving proteases. The enzymes process clinically relevant substrates such as Amyloid Precursor Protein (APP) and NOTCH and have been explored as drug targets in Alzheimer's disease, cancer, and other disorders (1). However, the clinical use of γ -secretase inhibitors (GSIs) has been hampered by severe mechanism-based dose-limiting toxicity; predominantly intestinal goblet cell hyperplasia and concomitant severe diarrhea (2), thymus atrophy and ablated T cell development (3, 4), splenic marginal zone atrophy (5), and skin lesions (6). This toxicity is due to systemic NOTCH inhibition because NOTCH receptors require γ -secretase complex-mediated processing for the release and nuclear translocation of the NOTCH intracellular domain (NICD) to activate gene expression (7).

It is, however, important to realize that the enzymatic activity of the γ -secretase complex reflects the combined activity of at least four different complexes. Clinical trials have been performed with broad-

spectrum, non-selective γ -secretase inhibitors that target all four complexes equally. The question remains whether inhibition of some but not all γ -secretase complexes, by subunit-selective targeting, could provide a way forward to safe targeting.

The four different γ -secretase complexes each contain one Nicastrin (NCSTN) and one Presenilin enhancer 2 (PEN-2) subunit. In addition, two different APH-1 proteins, APH-1A or APH-1B, and two different Presenilin (PSEN) proteins, PSEN1 or PSEN2, exist. One of the APH-1 and one of the PSEN proteins combine with the two stable subunits to generate four subcomplexes, which differ in their PSEN subunit and/or APH-1 subunit (8, 9). Different γ -secretase complexes can be expressed simultaneously by the same cells and at the same time (1, 10), but differ in their subcellular distribution and their biological function (11-13). Indeed, gene targeting of the different complexes revealed a variety of different outcomes, ranging from very severe embryonic lethal phenotypes (7, 14-16), to subtle behavioral phenotypes (17, 18), to normal mice (19).

The γ -secretase complexes have been mainly investigated in the context of Alzheimer's Disease because they process the Amyloid Precursor Protein (APP) to generate different amyloid- β profiles (12). Additionally, γ -secretase inhibitors have been investigated as targeted therapeutics for T cell acute lymphoblastic leukemia (T-ALL) (20), an aggressive hematologic malignancy resulting from the transformation of immature T cell progenitors (21, 22). In T-ALL, activating *NOTCH1* mutations are the most common mutations observed, present in approximately 60% of all cases (23-25). These mutations result in increased and ligand-independent oncogenic NOTCH1 signaling, promoting T cell transformation through the physiologic functions of NOTCH1 in the thymus (24, 26). However, like physiologic NOTCH1 signaling, oncogenic mutant NOTCH1 signaling still requires γ -secretase processing for activation, providing the rationale for GSIs as a therapeutic approach for T-ALL (20, 27-29).

Beyond T-ALL, increasing evidence is supporting a pathogenic role for NOTCH gain-of-function mutations in solid tumors. These cancers often display inappropriate NOTCH signaling due to overexpression of NOTCH receptors and/or ligands or loss of negative regulation of NOTCH signaling (30). Because of this, γ -secretase inhibitors were also investigated for a number of hematological and solid cancers, including breast cancer, pancreatic cancer, glioma, non-small cell lung cancer, and colorectal cancer (30). However, despite extensive research to develop several classes of GSIs, none of them sufficiently spared physiologic NOTCH signaling, and none of these drugs was successful in clinical trials (6). This has resulted in a halt to the therapeutic development of γ -secretase inhibitors in these areas. The hypothesis that selective inhibition of one of the γ -secretase complexes alone, targeting the enzyme most active in tumors while sparing other γ -secretase complexes in the hope of preserving physiological NOTCH signaling in the healthy tissues, has not been tested, however.

Here, we wanted to address whether selective γ -secretase inhibition could be a valid therapeutic approach. Given the high frequency of *NOTCH1* mutations that result in ligand-independent, but γ -secretase-dependent signaling in T-ALL, this cancer provides a perfect model to evaluate this hypothesis. We selectively targeted the PSEN1-containing γ -secretase complexes, while leaving the PSEN2-containing complexes untargeted. By doing so, we observed therapeutic efficacy against T-ALL, without the toxicity inherent to broad-spectrum GSIs.

Results

Presenilin-1 is highly expressed in T-ALL and regulates NOTCH1 cleavage

The Presenilin subunits PSEN1 or PSEN2 provide the catalytic center of the different γ -secretase complexes (**Fig. 1A**). Microarray analysis revealed that both *PSEN1* and *PSEN2* are expressed during human T cell development (69), although *PSEN1* has about four-fold higher expression compared to *PSEN2* (**Fig. 1B**). However, *PSEN1* expression is >30-fold higher than *PSEN2* expression in T-ALL cell lines and primary T-ALL patient samples (31, 32) (**Fig. 1C**). NOTCH1 signaling is essential for early T cell development in both mice and humans (26, 33), therefore we examined whether *Psen1* loss would abrogate normal T cell development in mice. Previously, a conditional *Psen1* knockout mouse was generated by targeting exon 2/3 (34). We developed a conditional *Psen1* knockout mouse targeting exon 1, using a DNA construct that also contained a tag (*Psen1^{ff}*) (**fig. S1A**), and then crossed it with a *CD2Cre* transgenic mouse (35) to inactivate *Psen1* in developing T cells (*CD2CrePsen1^{ΔΔ}* mice). The introduction of LoxP sites and a tag into the *Psen1* gene locus alone caused a 50% decrease in PSEN1 protein expression in thymocytes, but did not result in major T cell defects (**Fig. 1D-F**; **fig. S1B-D**). Notably, the complete loss of PSEN1 expression in thymocytes of *CD2CrePsen1^{ΔΔ}* mice did not alter the frequency of major T cell populations in the thymus (**Fig. 1D-F**). Although a small compensatory increase of PSEN2 expression was seen after loss of PSEN1, this was insufficient to overcome the overall loss in γ -secretase complex formation assessed by the strong reduction in nicastrin maturation that otherwise only occurs when a functional complex is present (**fig. S1B,C**). To study the possible decrease in T cell proliferation, we generated ex vivo cultures of mouse pro-T cells derived from C57BL/6 wild type, *Psen1^{ff}*, or *CD2CrePsen1^{ΔΔ}* mice (**fig. S2A**). These pro-T cells are cultured on DLL4 (NOTCH1 ligand)-coated plates and are strictly dependent on DLL4-induced NOTCH signaling (36). Pro-T cells derived from *CD2CrePsen1^{ΔΔ}* mice showed comparable proliferation to controls (**Fig. 1G**), demonstrating that PSEN1 is dispensable for normal T cell development. Apparently, the presence of PSEN2 is sufficient to maintain adequate NOTCH signaling to support normal development.

We next investigated whether *Psen1* gene inactivation could affect processing of mutant forms of the NOTCH1 receptor found in T-ALL. We transduced the mouse pro-T cells established from C57BL/6 wild type, *Psen1^{ff}*, or *CD2CrePsen1^{ΔΔ}* mice with a constitutively active mutant NOTCH1 receptor,

containing a heterodimerization (HD) and PEST domain mutation (NOTCH1-L1601P- Δ P). This mutant NOTCH1 receptor provides a substrate for γ -secretase, which is independent of ligand stimulation (24). C57BL/6 wild type and *Psen1^{fl/fl}* derived pro-T cells transduced with mutant NOTCH1 receptors were able to survive and proliferate without DLL4, confirming that the NOTCH1-L1601P- Δ P mutant can signal in the absence of DLL4. PSEN1 deletion significantly ($P \leq 0.05$) reduced pro-T cell proliferation and survival of NOTCH1-L1601P- Δ P expressing cells (**Fig. 1H**) and decreased mutant NOTCH1 receptor processing and NICD1 formation (**Fig. 1I**). Taken together, these data indicate that loss of PSEN1 specifically reduces oncogenic NOTCH1 signaling in T cells, whilst having limited effect on physiologic DLL4-mediated NOTCH signaling.

Genetic deletion of PSEN1 prolongs survival in NOTCH1-induced T cell leukemia in vivo

Given that loss of PSEN1 perturbs the processing and downstream signaling of mutant NOTCH1 receptors involved in T-ALL, we next assessed whether *Psen1* deletion could also impair mutant NOTCH1-induced T-ALL development in vivo. To this end, we transplanted wild type C57BL/6 mice with syngeneic wild type C57BL/6, *Psen1^{fl/fl}*, or *CD2CrePsen1^{Δ/Δ}* hematopoietic progenitors, expressing equivalent amounts of Δ EGF-NOTCH1-L1601P- Δ P, inferred from the extent of GFP expression, after retroviral transduction. (**Fig. 2A,B; fig. S2B**). Mice transplanted with wild type or *Psen1^{fl/fl}* cells transduced with Δ EGF-NOTCH1-L1601P- Δ P showed circulating GFP⁺ CD4⁺CD8⁺ T cells at 6 weeks after transplantation, indicative of leukemia development (**Fig. 2C,D**). Notably, mice transplanted with *CD2CrePsen1^{Δ/Δ}* cells transduced with Δ EGF-NOTCH1-L1601P- Δ P were largely devoid of circulating GFP⁺ T cells at 6 weeks after transplantation. At 9 weeks, mice transplanted with wild type and *Psen1^{fl/fl}* cells displayed splenomegaly and thymic enlargement due to CD4⁺CD8⁺ leukemic cell infiltration, which was still absent in mice transplanted with *CD2CrePsen1^{Δ/Δ}* cells (**Fig. 2E,F; fig. S2C**). These differences were not due to impaired homing and engraftment after transplantation of the *CD2CrePsen1^{Δ/Δ}* hematopoietic progenitors (**fig. S2D**). Eventually, only 9 out of 17 mice transplanted with *CD2CrePsen1^{Δ/Δ}* progenitors developed CD4⁺CD8⁺ leukemia, with a median overall survival of 120 days compared to 73 and 72 days median survival in wild type and *Psen1^{fl/fl}* transplanted mice, respectively ($p < 0.0001$, **Fig. 2G,H**). These data show that deficiency of PSEN1 alone is sufficient to majorly affect murine T-ALL induction.

Next, we set out to elucidate whether *Psen1* loss in an already established leukemia could still impair disease progression. To this end, we generated inducible *Psen1* conditional knockouts by crossing *Psen1^{fl/fl}* to *Rosa26Cre-ER^{T2}* mice, producing *R26Cre-ER^{T2}Psen1^{fl/fl}* mice. C57BL/6 mice were then transplanted with *R26Cre-ER^{T2}Psen1^{fl/fl}* hematopoietic progenitors transduced with Δ EGF-NOTCH1-L1601P- Δ P. After successful engraftment, *Psen1* was specifically deleted in transplanted donor cells through tamoxifen treatment (100 mg/kg for 5 days). These experiments were performed in primary recipient mice and were also repeated in tertiary transplanted recipient mice to assess whether loss of

PSEN1 in an aggressive leukemia setting still hampers disease progression (**Fig. 3A**). Analysis of *R26Cre-ER^{T2}Psen1^{ff}* leukemic cells recovered after tamoxifen treatment showed complete ablation of PSEN1 (**fig. S3A**). Specific *Psen1* deletion in the donor cells reduced leukemia burden, assessed by the fraction of circulating GFP⁺ cells in the peripheral blood, by two-fold at 5 weeks after transplantation and >6-fold at 9 weeks after transplantation in the primary recipient mice, compared to vehicle-treated mice (**Fig. 3B**). One week after tamoxifen treatment, analysis of age-matched mice showed that *Psen1* deletion reduced splenomegaly by 50% compared to vehicle-treated mice (**Fig. 3C**). Furthermore, *Psen1* deletion by tamoxifen treatment in an established leukemia increased the median overall survival to 142 days compared to 84.5 days for vehicle-treated mice ($p < 0.0001$, **Fig. 3D**). The tamoxifen-treated mice that did develop leukemia had lost PSEN1, excluding the possibility of having escaped recombination, but did show robust PSEN2 expression (**fig. S3B**). Tamoxifen treatment had no effect on leukemia progression and overall survival in mice transplanted with wild type C57BL/6 tumor cells expressing *Psen1* endogenously, compared to vehicle controls (**fig. S3C**).

Finally, we tested whether *Psen1* was required for leukemia maintenance and progression by targeting *Psen1* in a more aggressive and developed leukemia. Tertiary recipients were transplanted with leukemic cells from mice that suffered from full-blown leukemia, and these tertiary recipients were treated with vehicle or tamoxifen. Even in this aggressive leukemia model, *Psen1* deletion significantly increased survival ($p < 0.001$, **Fig. 3E**). Taken together, these data show the importance of PSEN1 in leukemia development and maintenance and validate PSEN1 as a potential target for therapy in T-ALL with NOTCH1 mutations.

Pharmacologic inhibition of PSEN1 impairs leukemia progression and prolongs survival in vivo

The decrease in leukemic burden identified through genetic loss of *Psen1* prompted us to investigate whether selective pharmacological PSEN1 inhibition would be a viable strategy for T-ALL treatment. To this end, we tested whether the PSEN1-selective inhibitor MRK-560, which has ~100-fold selectivity for PSEN1 over PSEN2 (37) (**fig. S4**), could block mutant NOTCH1 receptor signaling in human T-ALL cell lines. Indeed, MRK-560 treatment reduced NICD1 generation in HPB-ALL, DND-41, and Jurkat cell lines and resulted in a dose-dependent decrease of proliferation in HPB-ALL and DND-41, which depend on NOTCH signaling for their survival (**Fig. 4A,B**). Jurkat T-ALL cells harbor a *PTEN* deletion and are not dependent on NOTCH signaling for their proliferation, which explains why these cells do not show a decrease in survival upon MRK-560 treatment (28, 38, 39) (**Fig. 4B; table S1**). The effect of the PSEN1-selective γ -secretase inhibitor MRK-560 on proliferation could be attributed to a block in cell cycle (**Fig. 4C,D**).

Next, we determined whether pharmacological PSEN1 inhibition impaired T-ALL in vivo. Δ EGF-NOTCH1-L1601P- Δ P T-ALL lymphoblasts were injected into secondary recipients and treated with 30 μ mol/kg MRK-560 or vehicle for 14 days. MRK-560 treatment resulted in strong anti-leukemic effects

and improved median survival to 30 days compared to 18 days in vehicle-treated mice ($p=0.0009$, **Fig. 4E**). These data show marked therapeutic effects for pharmacological PSEN1 inhibition in T-ALL models in vitro and in vivo.

Having validated selective PSEN1 inhibition in a NOTCH1-driven mouse leukemia model, we next investigated the efficacy of PSEN1 targeting in human patient-derived xenograft (PDX) in vivo models. Immunodeficient NSG mice were injected with four genetically different PDX T-ALL samples with different *NOTCH1* mutations (**table S1**). Mice were randomized into vehicle and MRK-560 treatment arms and were treated with 30 $\mu\text{mol/kg}$ MRK-560 or vehicle for 14 days by subcutaneous injection. MRK-560 treatment significantly reduced leukemia burden compared to vehicle-treated mice, as assessed by peripheral blood counts of human CD45⁺ cells and in vivo bioluminescence ($P \leq 0.01$) (**Fig. 5A-D; fig. S5A-B**). The various degrees of response to MRK-560 treatment were not explained by differences in *PSEN1* expression in the PDX models (**fig. S5C**).

Analysis of age-matched vehicle- versus MRK-560-treated mice at the end of a 2-week treatment period showed up to 60% reduction in splenomegaly and up to 40% reduction in leukemic cell infiltration in the spleens of MRK-560-treated mice (**Fig. 5E-G**). Human HLA staining revealed a marked reduction of human leukemia cells in the spleen of MRK-560-treated animals compared to vehicle-treated mice, associated with reduced Ki67 staining, in line with reduced leukemia burden and inhibition of proliferation (**fig. S5D,E**). Most importantly, MRK-560 treatment significantly prolonged survival compared to vehicle-treated mice in all three *NOTCH1* mutant T-ALL patient samples tested here (1.1 fold, $p=0.0001$ for 389E, 1.5 fold, $p=0.0011$ for XC63, and 1.6 fold, $p=0.0027$ for XC65; **Fig. 5H-J**). Notably, single agent MRK-560 treatment was still effective even when treatment was initiated in mice with a high leukemia burden (“curative setting”), which resembles the clinical setting where disease is only detected when blood counts start to change (**Fig. 5C,J**). In these conditions, we observed a 1.5-fold increased survival compared to vehicle-treated mice ($p=0.0011$; **Fig. 5J**). Moreover, relapsing mice also remained sensitive to a second round of MRK-560 treatment, indicating no short-term outgrowth of an overtly resistant leukemia clone (**fig. S5F**). Analysis of leukemic cells after MRK-560 treatment showed that canonical NOTCH target genes *MYC*, *DTX1*, and *NOTCH3* were downregulated in T-ALL cells from MRK-560-treated mice compared to vehicle-treated mice (**Fig. 5K**), confirming “on-target” effects for MRK-560.

Pharmacological PSEN1-selective targeting does not cause gastrointestinal toxicity or T cell developmental defect

The major hurdle in adopting γ -secretase inhibitors clinically has been the “on-target” NOTCH-related toxicity, resulting in severe gastrointestinal goblet cell hyperplasia or defective T cell development. Notably, treatment with the PSEN1-selective γ -secretase inhibitor MRK-560 did not cause any

pathological changes in the gastrointestinal architecture or increased numbers of secretory goblet cells, assessed by Periodic Acid-Schiff (PAS) staining (**Fig. 6A**). In contrast, treatment with the classical broad-spectrum γ -secretase inhibitor dibenzazepine (DBZ, 10 μ mol/kg) resulted in a 4-fold increase in the number of secretory goblet cells, characteristic of gastrointestinal toxicity due to systemic NOTCH inhibition, as previously reported (2). Moreover, 4-week treatment of wild type mice with intermitted dosing of DBZ, as described previously (40), was still more toxic compared to MRK-560 (**fig. S6**). The expression of *PSEN1* and *PSEN2* within the human small intestine is nearly equivalent (**Fig. 6B**), suggesting that in the absence of PSEN1, the activity of PSEN2 may be sufficient to maintain normal gastrointestinal physiology. Furthermore, immunophenotyping revealed no major defects in thymic T cell development in healthy C57BL/6 mice treated with MRK-560 for 14 days, with cells progressing normally into CD4⁺CD8⁺ T cells (**Fig. 6C-E**), in line with the genetics experiments shown in Figure 1. In contrast, mice treated with DBZ showed defective T cell development, evidenced by a marked reduction in CD4⁺CD8⁺ T cells and an increase in DN1 stage T cells, as previously reported (26) for classical γ -secretase inhibitors. Altogether, these data provide evidence for a clear therapeutic window for selective PSEN1 targeting in T-ALL.

Discussion

Activating *NOTCH1* mutations are found in approximately 60% of T-ALL patients and across all T-ALL subtypes (24, 31). Therefore, targeting NOTCH1 by using GSIs that block NOTCH processing and activation has been of continuing clinical interest in the treatment of T-ALL. The gastrointestinal toxicity inherent to general GSIs is partially ameliorated with intermittent dosing regimens; nonetheless, the most recent clinical trials were still halted prematurely due to severe adverse effects (2, 6, 41). Here, we deliver proof of concept that selective targeting of PSEN1 γ -secretase complexes provides a viable and attractive alternative therapeutic approach. Both genetic and pharmacological experiments showed consistently that PSEN1 targeting alone is sufficient to strongly mitigate leukemia development, both in mutant NOTCH1-driven leukemia mouse models and in human patient-derived xenograft models. Using a tamoxifen-inducible model for *Psen1* deletion, we showed that these effects were also observed when *Psen1* was targeted after leukemia had developed, which more closely resembles the clinical situation. Importantly, the beneficial effects of pharmacological PSEN1 targeting were also observed when treatment was initiated at high blast count, which is classified clinically as higher risk with worse prognosis (42, 43). These data show that selective targeting of PSEN1 γ -secretase complexes provides a potent approach with high anti-leukemic activity, comparable to complete γ -secretase inhibition (44). These data are supported by an earlier observation that PSEN1 is required for the development of a DLL4-driven T cell lymphoma on a PSEN2-null background (45). Although that work demonstrated that PSEN1 is necessary, it did not show that it is sufficient to inhibit PSEN1 alone to block the lymphoma. Some mice in our experiments, with confirmed PSEN1 deletion, still developed leukemia, likely due to the observed compensatory high PSEN2 expression in their cells. Therefore, although

PSEN2 is not expressed in human T-ALL, reactivation of PSEN2 expression might be a potential resistance mechanism. Similarly, γ -secretase inhibition can reduce the frequency of leukemic stem cells, because mutant NOTCH1 signaling plays an important role in their maintenance (46-49). Although not tested here, our findings suggest that selective PSEN1 targeting might also have the promise to target these quiescent and therapy-resistant cells, believed to be responsible for T-ALL relapse.

The selective pharmacological inhibition of PSEN1 did not result in gastrointestinal toxicity or T cell development defects in mice, unlike the adverse effects observed with complete γ -secretase inhibition by DBZ. Our work extends previous studies in Alzheimer's disease models, where selective γ -secretase inhibition was efficacious and tolerable, although treatment periods in these studies were much shorter than in the current work (37, 50). This lack of toxicity in vivo may be partially explained by the observation that *PSEN2* and *PSEN1* expression is more equivalent within the gastrointestinal tract and developing T cells compared to T-ALL cells. Indeed, *Psen2*-knockout mice exposed to MRK-560 did display gastrointestinal and thymus toxicity, comparable to full γ -secretase inhibition, indicating that PSEN2 is responsible for the protective effects (37). Thus, although PSEN2 is insufficient to compensate for *Psen1* deletion during development (15), sparing PSEN2 activity maintains physiologically relevant signaling in the gut and hematopoietic system during adult life. To confirm that PSEN2 activity can compensate for the lack of PSEN1 activity, future studies will require a complete selective genetic knockout of *Psen1* in the gut, for example using a villin-Cre mouse model. However, for all practical means, it is clear that PSEN1-selective inhibition is highly preferable to the broad-spectrum inhibition that is induced by the previously tested γ -secretase inhibitors. As shown above, in human T-ALL cells, *PSEN1* expression is much higher than *PSEN2* expression (**Fig. 1**), and *PSEN2* expression is likely too low to provide sufficient support for leukemia development. Measuring *PSEN1/2* expression in circulating T-ALL cells might be a helpful parameter to decide whether selective PSEN1 targeting might be beneficial. In addition, PSEN1 and PSEN2 complexes have different subcellular profiles, resulting in substrate selectivity due to differential compartmentalization (11). Therefore, the differential sensitivity for leukemic cells versus normal tissue observed with the PSEN1 inhibitor might also be partially explained by enzyme-substrate specificity due to different subcellular localization. Further work should determine whether mutant NOTCH1 is processed at the cell surface, where PSEN1 complexes are predominantly expressed, while wild type NOTCH1 is processed additionally in endocytic compartments, where PSEN2 complexes reside (11).

Our study was conducted using preclinical experimental models that may not completely recapitulate their human counterparts. The murine leukemia models used were solely driven by mutant NOTCH1 signaling, whereas patients diagnosed with leukemia often display multiple different genetic lesions. However, the four human PDX samples used to determine the potency of pharmacological PSEN1-selective targeting displayed various mutational backgrounds, strengthening our preclinical findings. In

addition, human PDX models have shown concordance between preclinical results and corresponding available clinical data (51), making them a good model to study potential therapeutic approaches. Moreover, the overall increased safety profile of selective PSEN1 γ -secretase inhibition warrants optimism for further clinical development. Careful monitoring of thymus, gastrointestinal tract, and also skin, which is susceptible to tumorigenesis when *Psen1* is deleted (6, 52), will be necessary when further addressing the clinical feasibility of PSEN1 selective targeting in patients.

Finally, if further proof of concept can be established in T-ALL patients, even more applications for selective γ -secretase inhibition in the clinic could be envisaged. Indeed, safe selective γ -secretase inhibition might be useful as additional therapy in a variety of other cancers with deregulated NOTCH signaling, such as B cell lymphoma, breast cancer, and glioma (53-55). Furthermore, clinical interest in γ -secretase inhibition might become revived in other therapeutic areas where development was stopped because of gastrointestinal side effects, such as acute hearing loss (56, 57), peritoneal fibrosis as a complication of dialysis in renal disease (58), and atherosclerosis (59, 60).

Materials and Methods

Study design. We hypothesized that selective targeting of specific γ -secretase subunits is a safe strategy to target *NOTCH1* mutant T cell acute lymphoblastic leukemia. Cell culture experiments using cell lines were performed at least three times. Ex vivo T cell cultures were performed using at least three different mice to generate pro-T cells, unless otherwise noted. For treatment studies involving mice, disease burden was determined at treatment initiation, and animals were rank-ordered and divided into treatment arms after assuring that mean disease burden was comparable among groups. For toxicity studies in mice, animals were randomly assigned to treatment groups. Sample sizes for in vivo experiments were chosen based on previous experience and power calculations of expected differences with this type of experiments. Initial bone marrow transplants were replicated to test for variation in leukemia progression among different experiments. After this was ruled out, bone marrow transplantation experiments were no longer replicated, but sample size was large and results were reproducible among animals. For testing the effect of MRK-560 on human PDX samples in mice, every experiment was performed only once with five mice per treatment intervention. However, four independent PDX samples were chosen to ensure reproducibility among different patient samples to test for a broader applicability of the approach. Once conditions for an experiment were optimized, all data were included in the absence of a specific technical or procedural reason that confounded the interpretation of a finding. For bioluminescence imaging, the value from one vehicle-treated mouse on day 21 was excluded from the analysis, for technical reasons due to an incorrect IP injection. Bioluminescence values for this mouse before and after day 21 are present in the analysis. For histological analysis of intestinal toxicity, investigators were

blinded during goblet cell counting. During data collection and analysis, investigators were blinded to group allocation.

Cell culture, expression plasmids, and retrovirus production. HPB-ALL, DND-41, and Jurkat cell lines were cultured in RPMI medium supplemented with 20% fetal bovine serum (FBS). HEK293T cells were cultured in RPMI medium supplemented with 10% FBS. Mouse embryonic fibroblasts (MEFs) knocked out for *Psen* and *Aph1* and rescued with *PSEN1* and *APH1A* or *PSEN2* and *APH1A* expression were described previously (12). MEFs were transduced with pMSCV-NOTCH1ΔE-RFP-puromycin viral vectors, and after puromycin selection, RFP-positive cells were selected through FACS sorting and cultured in DMEM/F12 medium supplemented with 10% FBS. All other constructs used were cloned into the pMSCV-IRES-GFP vector. Viral vectors were produced in HEK293T cells using an EcoPack packaging plasmid and Genejuice transfection reagent (Merck-Millipore), and virus was harvested 48 hours after transfection. The stromal cell-free culture system used to generate mouse pro-T cells was described previously (61) and is summarized in supplementary materials and methods.

Compounds. DAPT was a kind gift from Janssen Pharmaceutica, and DBZ ((S)-2-(2-(3,5-Difluorophenyl)acetamido)-N-((S)-5-methyl-6-oxo-6,7-dihydro-5H-dibenzo[b,d]azepin-7-yl)propanamide) was purchased from Selleckchem. Dimethylsulfoxide (DMSO) was purchased from VWR, and (2-Hydroxypropyl)-β-cyclodextrin, meglumine, corn oil, and tamoxifen were purchased from Sigma-Aldrich. MRK-560 (*N*-[4-(4-chlorophenyl)sulfonyl-4-(2,5-difluorophenyl)cyclohexyl]-1,1,1-trifluoro methanesulfonamide) was kindly provided by Janssen Pharmaceutica and synthesized as described in supplementary materials and methods (62).

Gene expression profiling. Human thymocytes were extracted from thymus tissue from children undergoing cardiac surgery and were obtained and used according to the guidelines of the Medical Ethical Commission of the Ghent University Hospital, Belgium (Approval B670201319452). Fluorescence-activated cell sorter (FACS)-mediated cell sorting was used to isolate the different thymocyte subsets, representing the different stages of normal T cell development, as described previously (63, 64).

Mice and animal procedures. All experiments were approved by the Ethical Committee on Animal Experimenting of the University of Leuven. *Psen1* conditional knockout mice (*Psen1tm2.1Bdes*) were generated by homologous recombination in E14 ES cell line by introducing two loxP sites flanking exon 1. The first loxP site was introduced in intron 1 and the second together with a Frt-flanked hygromycin B selection marker cassette in intron 2. In addition, a double tag encoding calmodulin-binding protein (CBP) and 3xFLAG was inserted immediately after the ATG start codon. F1 offspring were crossed with *Gt(ROSA)26Sortm1(FLP1)Dym* strain and deletion of the selection cassette was confirmed by

Southern Blotting and PCR analysis. To generate mice carrying a *Psen1* deletion in all committed B and T cell progenitors, we crossed the mice harboring the conditional *Psen1* targeted allele with a specific Cre deleter line *B6.Cg-Tg(CD2-icre)4Kio/J* (The Jackson Laboratory, #008520), generating *CD2CrePsen1^{Δ/Δ}* mice. To generate conditional inducible *Psen1* knockout mice, we bred animals harboring the conditional *Psen1* allele with *B6.129-Gt(ROSA)26Sortm1(cre/ERT2)Tyj/J* mice, which express a tamoxifen-inducible form of the Cre recombinase, generating *Rosa26Cre-ER²Psen1^{ff}* mice. All colonies were kept on an inbred C57Bl/6J background, which was also used for wild type control animals and recipient animals for primary and secondary transplants. *NOD.Cg-Prkdcid112rgtm1WjlH2-Ab1tm1Gru Tg(HLA-DRB1)31Dmz/Szj* (NSG) mice used for patient-derived xenograft experiments were purchased from Harlan Laboratories. During experiments mice were housed in individually ventilated cages enriched with wood-wool and shavings as bedding, given access to water and food ad libitum, and monitored daily.

Murine bone marrow transplantation. Bone marrow transplantation to generate the mouse model for Δ EGF-NOTCH1-L1601P- Δ P was performed as described (65). Briefly, 6- to 12-week-old male mice were sacrificed and bone marrow cells were harvested from femur and tibia. Lineage-negative cells were enriched by negative selection using biotinylated antibodies directed against non-hematopoietic stem cells and non-progenitor cells (CD5, CD11b, CD19, CD45R/B220, Ly6G/C(Gr-1), TER119, 7-4) and streptavidin-coated magnetic particles (RapidSpheres, STEMCELL Technologies) and cultured overnight in RPMI with 20% FCS with IL-3 (10 ng/ml, Peprotech), IL-6 (10 ng/ml, Peprotech), SCF (50 ng/ml, Peprotech), and penicillin-streptomycin. The following day, 1×10^6 cells were transduced by spinoculation (90 min at 2500 rpm) with viral supernatant (Δ EGF-NOTCH1-L1601P- Δ P) and 8 μ g/ml polybrene. The following day, the cells were washed in PBS and injected (1×10^6 cells/0.3 ml) into the lateral tail vein of sublethally irradiated (5 Gy) syngeneic 8- to 12-week-old female C57BL/6 recipient mice. For secondary transplants, leukemic T cells were obtained from splenic tissue derived from mice transplanted with Δ EGF-NOTCH1-L1601P- Δ P wild type cells. After isolation, 1,000,000 cells were transplanted intravenously into sublethally irradiated (2.5 Gy) 8- to 10-week-old wild type (C57BL/6) female recipient mice. To delete the *Psen1* gene in NOTCH1-induced mouse leukemia, animals were treated with 100 mg/kg tamoxifen by IP injection for 5 consecutive days.

Human primary leukemia samples. Clinical leukemia samples were obtained with informed consent at local institutions and all experiments were conducted on protocols approved by the Ethical Committee of the University of Leuven.

In vivo imaging. For in vivo bioimaging, cells from NOTCH1 mutant T-ALL sample XC63 were injected into the tail vein of 6- to 12-week-old NSG mice, and human leukemic cell expansion was monitored through hCD45 staining on peripheral blood samples. After successful engraftment and

leukemic disease development, mice were sacrificed and single cells were isolated from the spleen, containing >90% hCD45⁺ cells. Splenocytes were transduced overnight with lentivirus pCH-SFFV-eGFP-P2A- β Luc and GFP-positive cells were sorted using a S3 Sorter (Bio-Rad) before being transplanted back into NSG mice via tail vein injection. Upon confirmation that leukemic cells were >95% GFP-positive, leukemic cells were isolated from the spleen and re-transplanted into a larger cohort of NSG mice for treatment studies. For in vivo bioluminescence imaging, anesthesia was induced in an induction chamber with 2% isoflurane in 100% oxygen at a flow rate of 2 l/min and maintained in the IVIS with a 1.5% mixture at 0.5 l/min. Before each imaging session, the mice were injected subcutaneously with 126 mg/kg d-luciferin (Promega, Leiden, the Netherlands) dissolved in PBS (15 mg/ml). Next, they were positioned in the IVIS and consecutive 2 min frames were acquired until the maximum signal was reached. Data are reported as the total flux per second from the whole mouse.

Toxicity studies, immunohistochemistry, immunofluorescence and flow cytometry. Healthy 12-week-old C57BL/6 mice were treated for 14 days with vehicle (20% hydroxypropyl- β -cyclodextrin (HP β CD) in 0.1 M meglumine) or 30 μ mol/kg MRK-560 by subcutaneous injection or 10 μ mol/kg DBZ or vehicle (0.5% methylcellulose, 0.1% Tween80) by IP injection. For the intermittent 4-week treatment, C57BL/6 mice were treated with the same concentrations of DBZ and MRK-560 but at a 5-day on/2-day off schedule. After treatment, thymus was isolated and single cells were prepared and stained for CD4, CD8, CD44 and CD25 to assess T cell development. To assess goblet cell hyperplasia, intestines from treated NSG mice were harvested and flushed with PBS and 10% neutral buffered formalin before fixation. For every mouse, a minimal of 10 villi were assessed for the number of secretory goblet cells. In addition, total body weight from all treated mice was assessed during and after treatment.

Patient-derived xenografts. Human leukemic bone marrow cells from NOTCH1 mutant T-ALL patients 389E, XC63, XC65, and XB47 (**table S1**) were injected into the tail vein of 6- to 12-week-old female NOD.Cg-Prkdc^{scid} Il2rg^{tm1Wjl}/SzJ (NSG) mice. After successful engraftment, splenocytes were harvested and reinjected at a concentration of 1×10^6 cells into secondary recipient NSG mice to create secondary transplants. Human leukemic cells were identified in peripheral blood samples by anti-hCD45 (APC, eBioscience) staining by flow cytometry or by luciferase in vivo bioimaging using the IVIS Spectrum (Caliper Lifesciences). After the leukemic clone was detectable in the blood or by bioimaging, mice were segregated randomly into treatment groups and treated daily for 14 days with vehicle or MRK-560 (30 μ mol/kg) dissolved in 20% hydroxypropyl- β -cyclodextrin (HP β CD) in 0.1 M meglumine by subcutaneous injection.

Statistical analyses. All analyses were performed using GraphPad Prism. Comparisons between two groups were performed by the Student's unpaired two-tailed t test. One-way analysis of variance (ANOVA) was used to examine differences when comparing effects in three groups, namely comparing

wild type, *Psen1^{ff}*, and *CD2CrePsen1^{Δ/Δ}* for leukemia progression, T cell development, and in ex vivo T cell cultures. For comparison of cell growth of T-ALL cells or leukemia progression in patient-derived xenograft models over time, differences were assessed by two-way ANOVA. Tukey post-hoc analysis was performed to correct for multiple comparisons. Survival in mouse experiments was represented with Kaplan-Meier survival curves and statistical significance was calculated using the log-rank test.

List of Supplementary Materials

Supplementary Materials and Methods

Fig. S1. *Psen1* deletion does not affect T cell development.

Fig. S2. *Psen1* deletion does not affect engraftment in bone marrow transplants.

Fig. S3. Tamoxifen does not affect leukemia progression

Fig. S4. MRK-560 shows selectivity for PSEN1 over PSEN2.

Fig. S5. Treatment of patient-derived xenograft samples with MRK-560

Fig. S6. Long term treatment with MRK-560 leads to significantly less gastrointestinal toxicity compared to DBZ

Table S1. T-ALL patient-derived xenograft samples

Table S2. Primers used for qPCR

References and notes

1. N. Jurisch-Yaksi, R. Sannerud, W. Annaert, A fast growing spectrum of biological functions of γ -secretase in development and disease, *Biochim. Biophys. Acta* **1828**, 2815–27 (2013).
2. J. H. van Es, M. E. van Gijn, O. Riccio, M. van den Born, M. Vooijs, H. Begthel, M. Cozijnsen, S. Robine, D. J. Winton, F. Radtke, H. Clevers, Notch/ γ -secretase inhibition turns proliferative cells in intestinal crypts and adenomas into goblet cells, *Nature* **435**, 959–963 (2005).
3. P. Doerfler, M. S. Shearman, R. M. Perlmutter, Presenilin-dependent gamma-secretase activity modulates thymocyte development, *Proc. Natl. Acad. Sci. U.S.A.* **98**, 9312–7 (2001).
4. G. T. Wong, D. Manfra, F. M. Poulet, Q. Zhang, H. Josien, T. Bara, L. Engstrom, M. Pinzon-Ortiz, J. S. Fine, H. J. Lee, L. Zhang, G. A. Higgins, E. M. Parker, Chronic treatment with the gamma-secretase inhibitor LY-411,575 inhibits beta-amyloid peptide production and alters lymphopoiesis and intestinal cell differentiation, *J. Biol. Chem.* **279**, 12876–82 (2004).
5. M. C. de Vera Mudry, F. Regenass-Lechner, L. Ozmen, B. Altmann, M. Festag, T. Singer, L. Müller, H. Jacobsen, A. Flohr, Morphologic and functional effects of gamma secretase inhibition on splenic marginal zone B cells, *Int J Alzheimers Dis* **2012**, 289412 (2012).
6. R. S. Doody, R. Raman, M. Farlow, T. Iwatsubo, B. Vellas, S. Joffe, K. Kieburtz, F. He, X. Sun, R. G. Thomas, P. S. Aisen, E. Siemers, G. Sethuraman, R. Mohs, A. D. C. S. S. Committee, S. S. Group,

- A phase 3 trial of semagacestat for treatment of Alzheimer's disease, *N. Engl. J. Med.* **369**, 341–50 (2013).
7. B. De Strooper, W. Annaert, P. Cupers, P. Saftig, K. Craessaerts, J. S. Mumm, E. H. Schroeter, V. Schrijvers, M. S. Wolfe, W. J. Ray, A. Goate, R. Kopan, A presenilin-1-dependent gamma-secretase-like protease mediates release of Notch intracellular domain, *Nature* **398**, 518–22 (1999).
 8. W. T. Kimberly, M. J. LaVoie, B. L. Ostaszewski, W. Ye, M. S. Wolfe, D. J. Selkoe, Gamma-secretase is a membrane protein complex comprised of presenilin, nicastrin, Aph-1, and Pen-2, *Proc. Natl. Acad. Sci. U.S.A.* **100**, 6382–7 (2003).
 9. B. De Strooper, Aph-1, Pen-2, and Nicastrin with Presenilin generate an active gamma-Secretase complex, *Neuron* **38**, 9–12 (2003).
 10. S. S. Hébert, L. Serneels, T. Dejaegere, K. Horr , M. Dabrowski, V. Baert, W. Annaert, D. Hartmann, B. De Strooper, Coordinated and widespread expression of gamma-secretase in vivo: evidence for size and molecular heterogeneity, *Neurobiol Dis* **17**, 260–72 (2004).
 11. R. Sannerud, C. Esselens, P. Ejsmont, R. Mattera, L. Rochin, A. K. Tharkeshwar, G. De Baets, V. De Wever, R. Habets, V. Baert, W. Vermeire, C. Michiels, A. J. Groot, R. Wouters, K. Dillen, K. Vints, P. Baatsen, S. Munck, R. Derua, E. Waelkens, G. S. Basi, M. Mercken, M. Vooijs, M. Bollen, J. Schymkowitz, F. Rousseau, J. S. Bonifacino, G. Van Niel, B. De Strooper, W. Annaert, Restricted Location of PSEN2/ γ -Secretase Determines Substrate Specificity and Generates an Intracellular A β Pool, *Cell* **166**, 193–208 (2016).
 12. H. Acx, L. Ch vez-Guti rrez, L. Serneels, S. Lismont, M. Benurwar, N. Elad, B. De Strooper, Signature amyloid β profiles are produced by different γ -secretase complexes, *Journal of Biological Chemistry* **289**, 4346–55 (2014).
 13. H. Acx, L. Serneels, E. Radaelli, S. Muyldermans, C. Vincke, E. Pepermans, U. M ller, L. Ch vez-Guti rrez, B. De Strooper, Inactivation of γ -secretases leads to accumulation of substrates and non-Alzheimer neurodegeneration, *EMBO Mol Med* **9**, 1088–1099 (2017).
 14. Wong, P. C., H. Zheng, H. Chen, M. W. Becher, D. J. Sirinathsinghji, M. E. Trumbauer, H. Y. Chen, D. L. Price, L. H. Van der Ploeg, S. S. Sisodia, Presenilin 1 is required for Notch1 and DIII expression in the paraxial mesoderm, *Nature* **387**, 288–92 (1997).
 15. J. Shen, R. T. Bronson, D. F. Chen, W. Xia, D. J. Selkoe, S. Tonegawa, Skeletal and CNS defects in Presenilin-1-deficient mice, *Cell* **89**, 629–39 (1997).
 16. L. Serneels, T. Dejaegere, K. Craessaerts, K. Horr , E. Jorissen, T. Tousseyn, S. H bert, M. Coolen, G. Martens, A. Zwijsen, W. Annaert, D. Hartmann, B. De Strooper, Differential contribution of the three Aph1 genes to gamma-secretase activity in vivo, *Proc. Natl. Acad. Sci. U.S.A.* **102**, 1719–24 (2005).
 17. T. Dejaegere, L. Serneels, M. K. Sch fer, J. Van Biervliet, K. Horr , C. Depboylu, D. Alvarez-Fischer, A. Herreman, M. Willem, C. Haass, G. U. H glinger, R. D'Hooge, B. De Strooper,

- Deficiency of Aph1B/C-gamma-secretase disturbs Nrg1 cleavage and sensorimotor gating that can be reversed with antipsychotic treatment, *Proc. Natl. Acad. Sci. U.S.A.* **105**, 9775–80 (2008).
18. L. Serneels, J. Van Biervliet, K. Craessaerts, T. Dejaegere, K. Horr , T. Van Houtvin, H. Esselmann, S. Paul, M. K. Sch fer, O. Berezovska, B. T. Hyman, B. Sprangers, R. Sciot, L. Moons, M. Jucker, Z. Yang, May, P. C., E. Karran, J. Wiltfang, R. D'Hooge, B. De Strooper, gamma-Secretase heterogeneity in the Aph1 subunit: relevance for Alzheimer's disease, *Science* **324**, 639–42 (2009).
19. A. Herreman, D. Hartmann, W. Annaert, P. Saftig, K. Craessaerts, L. Serneels, L. Umans, V. Schrijvers, F. Checler, H. Vanderstichele, V. Baekelandt, R. Dressel, P. Cupers, D. Huylebroeck, A. Zwijsen, F. Van Leuven, B. De Strooper, Presenilin 2 deficiency causes a mild pulmonary phenotype and no changes in amyloid precursor protein processing but enhances the embryonic lethal phenotype of presenilin 1 deficiency, *Proc. Natl. Acad. Sci. U.S.A.* **96**, 11872–7 (1999).
20. T. Palomero, A. Ferrando, Oncogenic NOTCH1 control of MYC and PI3K: challenges and opportunities for anti-NOTCH1 therapy in T-cell acute lymphoblastic leukemias and lymphomas, *Clin. Cancer Res.* **14**, 5314–7 (2008).
21. T. Girardi, C. Vicente, J. Cools, K. De Keersmaecker, The genetics and molecular biology of T-ALL, *Blood* **129**, 1113–1123 (2017).
22. P. Van Vlierberghe, A. Ferrando, The molecular basis of T cell acute lymphoblastic leukemia, *J. Clin. Invest.* **122**, 3398–406 (2012).
23. W. S. Pear, J. C. Aster, M. L. Scott, R. P. Hasserjian, B. Soffer, J. Sklar, D. Baltimore, Exclusive development of T cell neoplasms in mice transplanted with bone marrow expressing activated Notch alleles, *J. Exp. Med.* **183**, 2283–91 (1996).
24. A. P. Weng, A. A. Ferrando, W. Lee, J. P. Morris, L. B. Silverman, C. Sanchez-Irizarry, S. C. Blacklow, A. T. Look, J. C. Aster, Activating mutations of NOTCH1 in human T cell acute lymphoblastic leukemia, *Science* **306**, 269–71 (2004).
25. M. R. Mansour, D. C. Linch, L. Foroni, A. H. Goldstone, R. E. Gale, High incidence of Notch-1 mutations in adult patients with T-cell acute lymphoblastic leukemia, *Leukemia* **20**, 537–9 (2006).
26. F. Radtke, A. Wilson, G. Stark, M. Bauer, J. van Meerwijk, H. R. MacDonald, M. Aguet, Deficient T cell fate specification in mice with an induced inactivation of Notch1, *Immunity* **10**, 547–58 (1999).
27. A. P. Weng, Y. Nam, M. S. Wolfe, W. S. Pear, J. D. Griffin, S. C. Blacklow, J. C. Aster, Growth suppression of pre-T acute lymphoblastic leukemia cells by inhibition of notch signaling, *Molecular and Cellular Biology* **23**, 655–64 (2003).
28. T. Palomero, M. L. Sulis, M. Cortina, P. J. Real, K. Barnes, M. Ciofani, E. Caparros, J. Buteau, K. Brown, S. L. Perkins, G. Bhagat, A. M. Agarwal, G. Basso, M. Castillo, S. Nagase, C. Cordon-Cardo, R. Parsons, J. C. Z niga-Pfl cker, M. Dominguez, A. A. Ferrando, Mutational loss of PTEN induces resistance to NOTCH1 inhibition in T-cell leukemia, *Nat. Med.* **13**, 1203–10 (2007).

29. P. J. Real, V. Tosello, T. Palomero, M. Castillo, E. Hernando, E. de Stanchina, M. L. Sulis, K. Barnes, C. Sawai, I. Homminga, J. Meijerink, I. Aifantis, G. Basso, C. Cordon-Cardo, W. Ai, A. Ferrando, Gamma-secretase inhibitors reverse glucocorticoid resistance in T cell acute lymphoblastic leukemia, *Nat. Med.* **15**, 50–8 (2009).
30. P. Ranganathan, K. L. Weaver, A. J. Capobianco, Notch signalling in solid tumours: a little bit of everything but not all the time, *Nat. Rev. Cancer* **11**, 338–51 (2011).
31. Y. Liu, J. Easton, Y. Shao, J. Maciaszek, Z. Wang, M. R. Wilkinson, K. McCastlain, M. Edmonson, S. B. Pounds, L. Shi, X. Zhou, X. Ma, E. Sioson, Y. Li, M. Rusch, P. Gupta, D. Pei, C. Cheng, M. A. Smith, J. G. Auvil, D. S. Gerhard, M. V. Relling, N. J. Winick, A. J. Carroll, N. A. Heerema, E. Raetz, M. Devidas, C. L. Willman, R. C. Harvey, W. L. Carroll, K. P. Dunsmore, S. S. Winter, B. L. Wood, B. P. Sorrentino, J. R. Downing, M. L. Loh, S. P. Hunger, J. Zhang, C. G. Mullighan, The genomic landscape of pediatric and young adult T-lineage acute lymphoblastic leukemia, *Nat. Genet.* **49**, 1211–1218 (2017).
32. Z. K. Atak, V. Gianfelici, G. Hulselmans, K. De Keersmaecker, A. G. Devasia, E. Geerdens, N. Mentens, S. Chiaretti, K. Durinck, A. Uyttebroeck, P. Vandenberghe, I. Wlodarska, J. Cloos, R. Foà, F. Speleman, J. Cools, S. Aerts, Comprehensive analysis of transcriptome variation uncovers known and novel driver events in T-cell acute lymphoblastic leukemia, *PLoS Genet.* **9**, e1003997 (2013).
33. E. Waegemans, I. Van de Walle, J. De Medts, M. De Smedt, T. Kerre, B. Vandekerckhove, G. Leclercq, T. Wang, J. Plum, T. Taghon, Notch3 activation is sufficient but not required for inducing human T-lineage specification, *J. Immunol.* **193**, 5997–6004 (2014).
34. H. Yu, C. A. Saura, S. Y. Choi, L. D. Sun, X. Yang, M. Handler, T. Kawarabayashi, L. Younkin, B. Fedeles, M. A. Wilson, S. Younkin, E. R. Kandel, A. Kirkwood, J. Shen, APP processing and synaptic plasticity in presenilin-1 conditional knockout mice, *Neuron* **31**, 713–726 (2001).
35. J. de Boer, A. Williams, G. Skavdis, N. Harker, M. Coles, M. Tolaini, T. Norton, K. Williams, K. Roderick, A. J. Potocnik, D. Kioussis, Transgenic mice with hematopoietic and lymphoid specific expression of Cre, *Eur. J. Immunol.* **33**, 314–25 (2003).
36. S. Bornschein, S. Demeyer, R. Stirparo, O. Gielen, C. Vicente, E. Geerdens, B. Ghesquière, S. Aerts, J. Cools, C. E. de Bock, Defining the molecular basis of oncogenic cooperation between TAL1 expression and Pten deletion in T-ALL using a novel pro-T-cell model system, *Leukemia* (2017), doi:10.1038/leu.2017.328.
37. T. Borgegård, S. Gustavsson, C. Nilsson, S. Parpal, R. Klintonberg, A. L. Berg, S. Rosqvist, L. Serneels, S. Svensson, F. Olsson, S. Jin, H. Yan, J. Wangren, A. Jureus, A. Ridderstad-Wollberg, P. Wollberg, K. Stockling, H. Karlström, A. Malmberg, J. Lund, P. I. Arvidsson, B. De Strooper, U. Lendahl, J. Lundkvist, Alzheimer's disease: presenilin 2-sparing γ -secretase inhibition is a tolerable A β peptide-lowering strategy, *J. Neurosci.* **32**, 17297–305 (2012).
38. Z. Kalender Atak, K. De Keersmaecker, V. Gianfelici, E. Geerdens, R. Vandepoel, D. Pauwels, M. Porcu, I. Lahortiga, V. Brys, W. G. Dirks, H. Quentmeier, J. Cloos, H. Cuppens, A. Uyttebroeck, P.

- Vandenbergh, J. Cools, S. Aerts, High accuracy mutation detection in leukemia on a selected panel of cancer genes, *PLoS ONE* **7**, e38463 (2012).
39. K. De Keersmaecker, I. Lahortiga, N. Mentens, C. Folens, L. Van Neste, S. Bekaert, P. Vandenbergh, M. D. Otero, P. Marynen, J. Cools, In vitro validation of gamma-secretase inhibitors alone or in combination with other anti-cancer drugs for the treatment of T-cell acute lymphoblastic leukemia, *Haematologica* **93**, 533–42 (2008).
40. D. Herranz, A. Ambesi-Impombato, J. Sudderth, M. Sanchez-Martin, L. Belver, V. Tosello, L. Xu, A. A. Wendorff, M. Castillo, J. E. Haydu, J. Márquez, J. M. Matés, A. L. Kung, S. Rayport, C. Cordon-Cardo, R. J. DeBerardinis, A. A. Ferrando, Metabolic reprogramming induces resistance to anti-NOTCH1 therapies in T cell acute lymphoblastic leukemia, *Nat. Med.* **21**, 1182–1189 (2015).
41. A. W. Tolcher, W. A. Messersmith, S. M. Mikulski, K. P. Papadopoulos, E. L. Kwak, D. G. Gibbon, A. Patnaik, G. S. Falchook, A. Dasari, G. I. Shapiro, J. F. Boylan, Z. X. Xu, K. Wang, A. Koehler, J. Song, S. A. Middleton, J. Deutsch, M. Demario, R. Kurzrock, J. J. Wheler, Phase I study of RO4929097, a gamma secretase inhibitor of Notch signaling, in patients with refractory metastatic or locally advanced solid tumors, *J. Clin. Oncol.* **30**, 2348–53 (2012).
42. M. Aricò, M. G. Valsecchi, B. Camitta, M. Schrappe, J. Chessells, A. Baruchel, P. Gaynon, L. Silverman, G. Janka-Schaub, W. Kamps, C.-H. Pui, G. Masera, Outcome of treatment in children with Philadelphia chromosome-positive acute lymphoblastic leukemia, *N. Engl. J. Med.* **342**, 998–1006 (2000).
43. J. M. Ribera, J. J. Ortega, A. Oriol, P. Bastida, C. Calvo, J. M. Pérez-Hurtado, M. E. González-Valentín, V. Martín-Reina, A. Molinés, F. Ortega-Rivas, M. J. Moreno, C. Rivas, I. Egurbide, I. Heras, C. Poderós, E. Martínez-Revuelta, J. M. Guinea, E. del Potro, G. Deben, Comparison of intensive chemotherapy, allogeneic, or autologous stem-cell transplantation as postremission treatment for children with very high risk acute lymphoblastic leukemia: PETHEMA ALL-93 Trial, *J. Clin. Oncol.* **25**, 16–24 (2007).
44. K. Cullion, K. M. Draheim, N. Hermance, J. Tammam, V. M. Sharma, C. Ware, G. Nikov, V. Krishnamoorthy, P. K. Majumder, M. A. Kelliher, Targeting the Notch1 and mTOR pathways in a mouse T-ALL model, *Blood* **113**, 6172–81 (2009).
45. H. Xiong, A. Maraver, J.-A. Latkowski, T. Henderson, K. Schlessinger, Y. Ding, J. Shen, C. E. Tadokoro, J. J. Lafaille, Characterization of two distinct lymphoproliferative diseases caused by ectopic expression of the Notch ligand DLL4 on T cells, *PLoS ONE* **8**, e84841 (2013).
46. B. Gerby, C. S. Tremblay, M. Tremblay, S. Rojas-Sutterlin, S. Herblot, J. Hébert, G. Sauvageau, S. Lemieux, E. Lécuyer, D. F. Veiga, T. Hoang, SCL, LMO1 and Notch1 reprogram thymocytes into self-renewing cells, *PLoS Genet.* **10**, e1004768 (2014).
47. S. Goossens, P. Van Vlierbergh, Controlling pre-leukemic thymocyte self-renewal, *PLoS Genet.* **10**, e1004881 (2014).

48. J. Tatarek, K. Cullion, T. Ashworth, R. Gerstein, J. C. Aster, M. A. Kelliher, Notch1 inhibition targets the leukemia-initiating cells in a Tal1/Lmo2 mouse model of T-ALL, *Blood* **118**, 1579–90 (2011).
49. F. Armstrong, P. Brunet de la Grange, B. Gerby, M. C. Rouyez, J. Calvo, M. Fontenay, N. Boissel, H. Dombret, A. Baruchel, J. Landman-Parker, P. H. Roméo, P. Ballerini, F. Pflumio, NOTCH is a key regulator of human T-cell acute leukemia initiating cell activity, *Blood* **113**, 1730–40 (2009).
50. J. D. Best, D. W. Smith, M. A. Reilly, R. O'Donnell, H. D. Lewis, S. Ellis, N. Wilkie, T. W. Rosahl, P. A. Laroque, C. Boussiquet-Leroux, I. Churcher, J. R. Atack, T. Harrison, M. S. Shearman, The novel gamma secretase inhibitor N-[cis-4-[(4-chlorophenyl)sulfonyl]-4-(2,5-difluorophenyl)cyclohexyl]-1,1,1-trifluoromethanesulfonamide (MRK-560) reduces amyloid plaque deposition without evidence of notch-related pathology in the Tg2576 mouse, *J Pharmacol Exp Ther* **320**, 552–8 (2007).
51. L. Jones, H. Carol, K. Evans, J. Richmond, P. J. Houghton, M. A. Smith, R. B. Lock, A review of new agents evaluated against pediatric acute lymphoblastic leukemia by the Pediatric Preclinical Testing Program, *Leukemia* **30**, 2133–2141 (2016).
52. X. Xia, S. Qian, S. Soriano, Y. Wu, A. M. Fletcher, X. J. Wang, E. H. Koo, X. Wu, H. Zheng, Loss of presenilin 1 is associated with enhanced beta-catenin signaling and skin tumorigenesis, *Proc. Natl. Acad. Sci. U.S.A.* **98**, 10863–8 (2001).
53. X. S. Puente, M. Pinyol, V. Quesada, L. Conde, G. R. Ordóñez, N. Villamor, G. Escaramis, P. Jares, S. Beà, M. González-Díaz, L. Bassaganyas, T. Baumann, M. Juan, M. López-Guerra, D. Colomer, J. M. Tubío, C. López, A. Navarro, C. Tornador, M. Aymerich, M. Rozman, J. M. Hernández, D. A. Puente, J. M. Freije, G. Velasco, A. Gutiérrez-Fernández, D. Costa, A. Carrió, S. Guijarro, A. Enjuanes, L. Hernández, J. Yagüe, P. Nicolás, C. M. Romeo-Casabona, H. Himmelbauer, E. Castillo, J. C. Dohm, S. de Sanjosé, M. A. Piris, E. de Alava, J. San Miguel, R. Royo, J. L. Gelpí, D. Torrents, M. Orozco, D. G. Pisano, A. Valencia, R. Guigó, M. Bayés, S. Heath, M. Gut, P. Klatt, J. Marshall, K. Raine, L. A. Stebbings, P. A. Futreal, M. R. Stratton, P. J. Campbell, I. Gut, A. López-Guillermo, X. Estivill, E. Montserrat, C. López-Otín, E. Campo, Whole-genome sequencing identifies recurrent mutations in chronic lymphocytic leukaemia, *Nature* **475**, 101–5 (2011).
54. I. Krop, T. Demuth, T. Guthrie, P. Y. Wen, W. P. Mason, P. Chinnaiyan, N. Butowski, M. D. Groves, S. Kesari, S. J. Freedman, S. Blackman, J. Watters, A. Loboda, A. Podtelezchnikov, J. Lunceford, C. Chen, M. Giannotti, J. Hing, R. Beckman, P. Lorusso, Phase I pharmacologic and pharmacodynamic study of the gamma secretase (Notch) inhibitor MK-0752 in adult patients with advanced solid tumors, *J. Clin. Oncol.* **30**, 2307–13 (2012).
55. A. F. Schott, M. D. Landis, G. Dontu, K. A. Griffith, R. M. Layman, I. Krop, L. A. Paskett, H. Wong, L. E. Dobrolecki, M. T. Lewis, A. M. Froehlich, J. Paratilam, D. F. Hayes, M. S. Wicha, J. C. Chang, Preclinical and clinical studies of gamma secretase inhibitors with docetaxel on human breast tumors, *Clin. Cancer Res.* **19**, 1512–24 (2013).

56. K. Mizutani, M. Fujioka, M. Hosoya, N. Bramhall, H. J. Okano, H. Okano, A. S. Edge, Notch inhibition induces cochlear hair cell regeneration and recovery of hearing after acoustic trauma, *Neuron* **77**, 58–69 (2013).
57. Y. Tona, K. Hamaguchi, M. Ishikawa, T. Miyoshi, N. Yamamoto, K. Yamahara, J. Ito, T. Nakagawa, Therapeutic potential of a gamma-secretase inhibitor for hearing restoration in a guinea pig model with noise-induced hearing loss, *BMC Neurosci* **15**, 66 (2014).
58. F. Zhu, T. Li, F. Qiu, J. Fan, Q. Zhou, X. Ding, J. Nie, X. Yu, Preventive effect of Notch signaling inhibition by a gamma-secretase inhibitor on peritoneal dialysis fluid-induced peritoneal fibrosis in rats, *Am J Pathol* **176**, 650–9 (2010).
59. T. Aoyama, K. Takeshita, R. Kikuchi, K. Yamamoto, X. W. Cheng, J. K. Liao, T. Murohara, gamma-Secretase inhibitor reduces diet-induced atherosclerosis in apolipoprotein E-deficient mice, *Biochem. Biophys. Res. Commun.* **383**, 216–21 (2009).
60. D. Fukuda, E. Aikawa, F. K. Swirski, T. I. Novobrantseva, V. Kotlianski, C. Z. Gorgun, A. Chudnovskiy, H. Yamazaki, K. Croce, R. Weissleder, J. C. Aster, G. S. Hotamisligil, H. Yagita, M. Aikawa, Notch ligand delta-like 4 blockade attenuates atherosclerosis and metabolic disorders, *Proc. Natl. Acad. Sci. U.S.A.* **109**, E1868–77 (2012).
61. N. Gehre, A. Nusser, L. von Muenchow, R. Tussiwand, C. Engdahl, G. Capoferri, N. Bosco, R. Ceredig, A. G. Rolink, A stromal cell free culture system generates mouse pro-T cells that can reconstitute T-cell compartments in vivo, *Eur. J. Immunol.* **45**, 932–42 (2015).
62. I. Churcher, D. Beher, J. D. Best, J. L. Castro, E. E. Clarke, A. Gentry, T. Harrison, L. Hitzel, E. Kay, S. Kerrad, H. D. Lewis, P. Morentin-Gutierrez, R. Mortishire-Smith, P. J. Oakley, M. Reilly, D. E. Shaw, M. S. Shearman, M. R. Teall, S. Williams, J. D. J. Wrigley, 4-substituted cyclohexyl sulfones as potent, orally active gamma-secretase inhibitors, *Bioorg. Med. Chem. Lett.* **16**, 280–284 (2006).
63. S. Peirs, F. Matthijssens, S. Goossens, I. Van de Walle, K. Ruggero, C. E. de Bock, S. Degryse, K. Canté-Barrett, D. Briot, E. Clappier, T. Lammens, B. De Moerloose, Y. Benoit, B. Poppe, J. P. Meijerink, J. Cools, J. Soulier, T. H. Rabbitts, T. Taghon, F. Speleman, P. Van Vlierberghe, ABT-199 mediated inhibition of BCL-2 as a novel therapeutic strategy in T-cell acute lymphoblastic leukemia, *Blood* **124**, 3738–47 (2014).
64. T. Taghon, E. Waegemans, I. Van de Walle, Notch signaling during human T cell development, *Curr. Top. Microbiol. Immunol.* **360**, 75–97 (2012).
65. C. E. de Bock, S. Demeyer, S. Degryse, D. Verbeke, B. Sweron, O. Gielen, R. Vandepoel, C. Vicente, M. Vanden Bempt, A. Dagklis, E. Geerdens, S. Bornschein, R. Gijssbers, J. Soulier, J. P. Meijerink, M. Heinäniemi, S. Teppo, M. Bouvy-Liivrand, O. Lohi, E. Radaelli, J. Cools, HOXA9 Cooperates with Activated JAK/STAT Signaling to Drive Leukemia Development, *Cancer Discov* **8**, 616–631 (2018).

66. W. G. Annaert, C. Esselens, V. Baert, C. Boeve, G. Snellings, P. Cupers, K. Craessaerts, B. De Strooper, Interaction with telencephalin and the amyloid precursor protein predicts a ring structure for presenilins, *Neuron* **32**, 579–89 (2001).
67. C. Esselens, V. Oorschot, V. Baert, T. Raemaekers, K. Spittaels, L. Serneels, H. Zheng, P. Saftig, B. De Strooper, J. Klumperman, W. Annaert, Presenilin 1 mediates the turnover of telencephalin in hippocampal neurons via an autophagic degradative pathway, *J. Cell Biol.* **166**, 1041–54 (2004).
68. P. Bankhead, M. B. Loughrey, J. A. Fernández, Y. Dombrowski, D. G. McArt, P. D. Dunne, S. McQuaid, R. T. Gray, L. J. Murray, H. G. Coleman, J. A. James, M. Salto-Tellez, P. W. Hamilton, QuPath: Open source software for digital pathology image analysis, *Sci Rep* **7**, 16878 (2017).
69. S. Peirs, F. Matthijssens, S. Goossens, I. Van de Walle, K. Ruggero, C. E. de Bock, S. Degryse, K. Canté-Barrett, D. Briot, E. Clappier, T. Lammens, B. De Moerloose, Y. Benoit, B. Poppe, J. P. Meijerink, J. Cools, J. Soulier, T. H. Rabbitts, T. Taghon, F. Speleman, P. Van Vlierberghe, ABT-199 mediated inhibition of BCL-2 as a novel therapeutic strategy in T-cell acute lymphoblastic leukemia, *Blood* **124**,

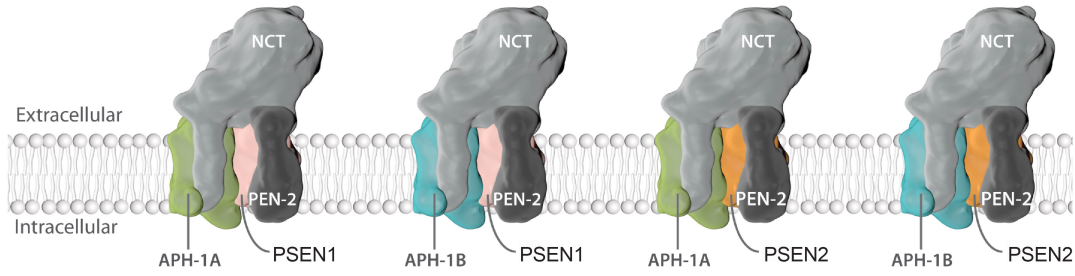
Acknowledgements

Synthesis of MRK-560 took place at Janssen Pharmaceutica Neuroscience Medicinal Chemistry by RN, as a visiting scientist. **Funding:** This work was supported by the Fonds voor Wetenschappelijk Onderzoek - Vlaanderen (FWO), the KU Leuven and VIB, a Methusalem grant from the KU Leuven/Flemish Government and Stichting Alzheimer Onderzoek (SAO) to BDS. BDS is supported by the Bax-Vanluffelen Chair for Alzheimer’s Disease, and “Opening the Future” of the Leuven Universiteit Fonds (LUF). JC is supported by an ERC-consolidator grant (617340) and “Kom op tegen Kanker” (stand up to cancer), the Flemish cancer society. RH is supported by a FWO fellowship (12I2317N). **Author contributions:** RAH, CEDB, JC and BDS conceived the study, designed and analyzed experiments and prepared the manuscript. RAH and CEDB performed most of the experiments with the help of DN, IL, DV, LS, JD and AL. SD performed analysis of RNA-seq data and TT performed analysis of Micro-Array data. RN performed MRK-560 synthesis. All authors reviewed the manuscript and agreed with the final submission. **Competing interests:** BDS and RN received a grant from Janssen Pharmaceutica for the development of γ -secretase inhibitors. The other authors declare that they have no competing interests. **Data and materials availability:** Data for PSEN1 and PSEN2 expression in human small intestine were obtained from the GTEx portal and dbGaP accession number phs000424.vN.pN. RNA-sequencing data on T-ALL cell lines are available in the EGA database with accession number EGAD00001000849. RNA-seq data for human T-ALL can be accessed at <https://ocg.cancer.gov/programs/target/data-matrix>.

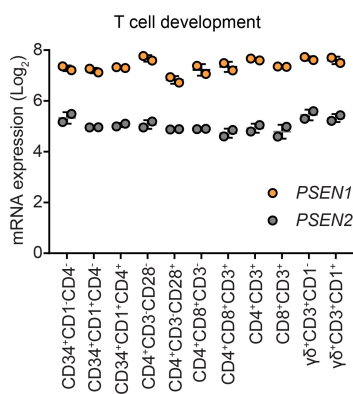
Figures

Fig. 1

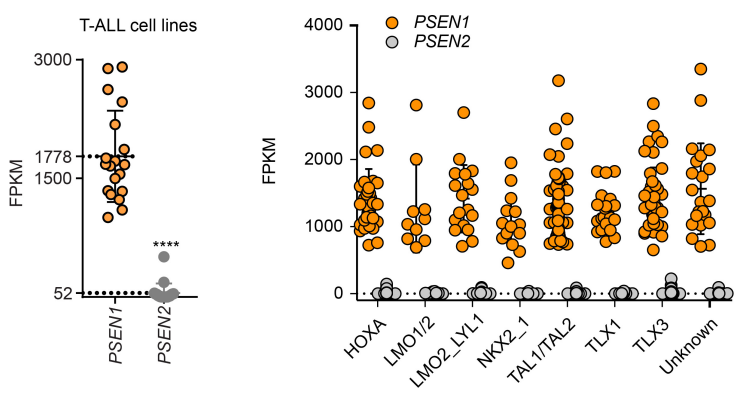
A



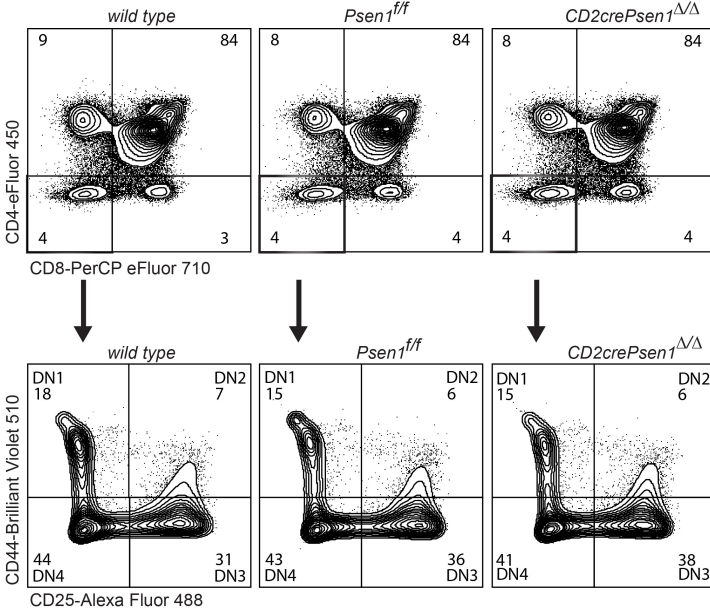
B



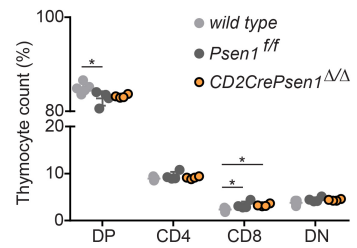
C



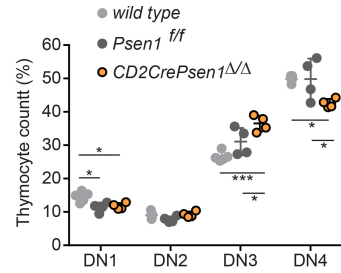
D



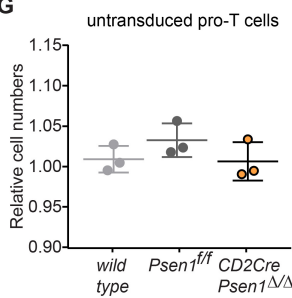
E



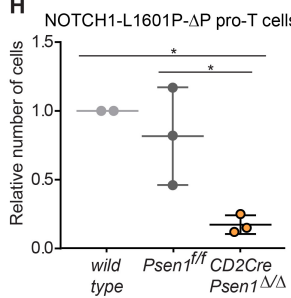
F



G



H



I

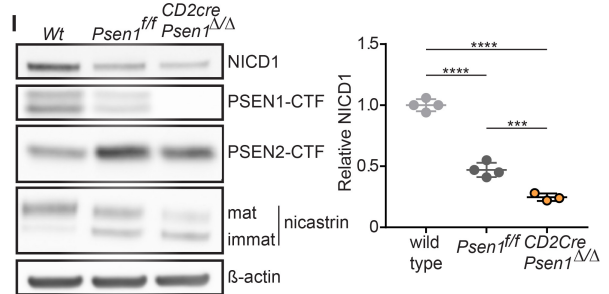


Fig. 1. PSEN1 deletion specifically reduces oncogenic mutant NOTCH1 signaling in T cells.

(A) Schematic representation of the four different γ -secretase complexes that exist in humans. All complexes contain nicastrin (NCT), Presenilin-enhancer-2 (PEN-2) and either APH-1A or APH-1B and PSEN1 or PSEN2. (B) *PSEN1* (probe X203460_s_at) and *PSEN2* (probe X211373_s_at) expression in sorted subsets of human thymocytes. Average expression and standard deviation in samples obtained from two different donors are shown. (C) RNA-sequencing FPKM *PSEN1* and *PSEN2* expression in T-ALL cell lines (ALL-SIL, CCRF-CEM, DND-41, HPB-ALL, HSB2, Jurkat, Karpas45, KE37, LOUCY, MOLT14, MOLT4, P12-Ichikawa, PEER, PF382, RPMI-8402, RM2, SUPT1, SUPT13, and T-ALL1) and T-ALL patient samples. (D) Representative flow cytometry plots of thymocyte populations stained with antibodies against CD4 and CD8 or CD44 and CD25 in C57BL/6 *wild type*, *Psen1^{ff}*, or *CD2CrePsen1^{Δ/Δ}* mice. (E) Quantification of mature thymic T cell populations in relative numbers (*wild type*: n=5, *Psen1^{ff}*: n=4, *CD2CrePsen1^{Δ/Δ}*: n=4). (F) Quantification of immature thymic T cell populations in relative numbers (*wild type*: n=5, *Psen1^{ff}*: n=4, *CD2CrePsen1^{Δ/Δ}*: n=4). (G) Relative cell numbers in ex vivo cultures of mouse pro-T cells derived from C57BL/6 *wild type*, *Psen1^{ff}*, or *CD2CrePsen1^{Δ/Δ}* mice and grown for 7 days (n=3 for all). (H) Relative cell numbers in ex vivo cultures of mouse pro-T cells derived from C57BL/6 *wild type* (n=2), *Psen1^{ff}* (n=3), or *CD2CrePsen1^{Δ/Δ}* (n=3) mice transduced with MSCV-NOTCH1-L1601P- Δ P-IRES-GFP and grown for 7 days without DLL4. (I) Western blot analysis of C57BL/6 *wild type* (n=4), *Psen1^{ff}* (n=4), or *CD2CrePsen1^{Δ/Δ}* (n=3) NOTCH1-L1601P- Δ P pro-T cells for NICD1, PSEN1, PSEN2, nicastrin, and β -actin cultured in the absence of DLL4 for 72 hours. Quantification of NICD1 expression is shown on the right. NICD1, NOTCH1 intracellular domain. All graphs show the mean values, and error bars represent standard deviation. P-values for C were calculated using two-tailed Student's t-test. **** $P \leq 0.0001$. P-values in E, F, G, H, and I were calculated using one-way ANOVA. * $P \leq 0.05$, *** $P \leq 0.001$ and **** $P \leq 0.0001$.

Fig. 2

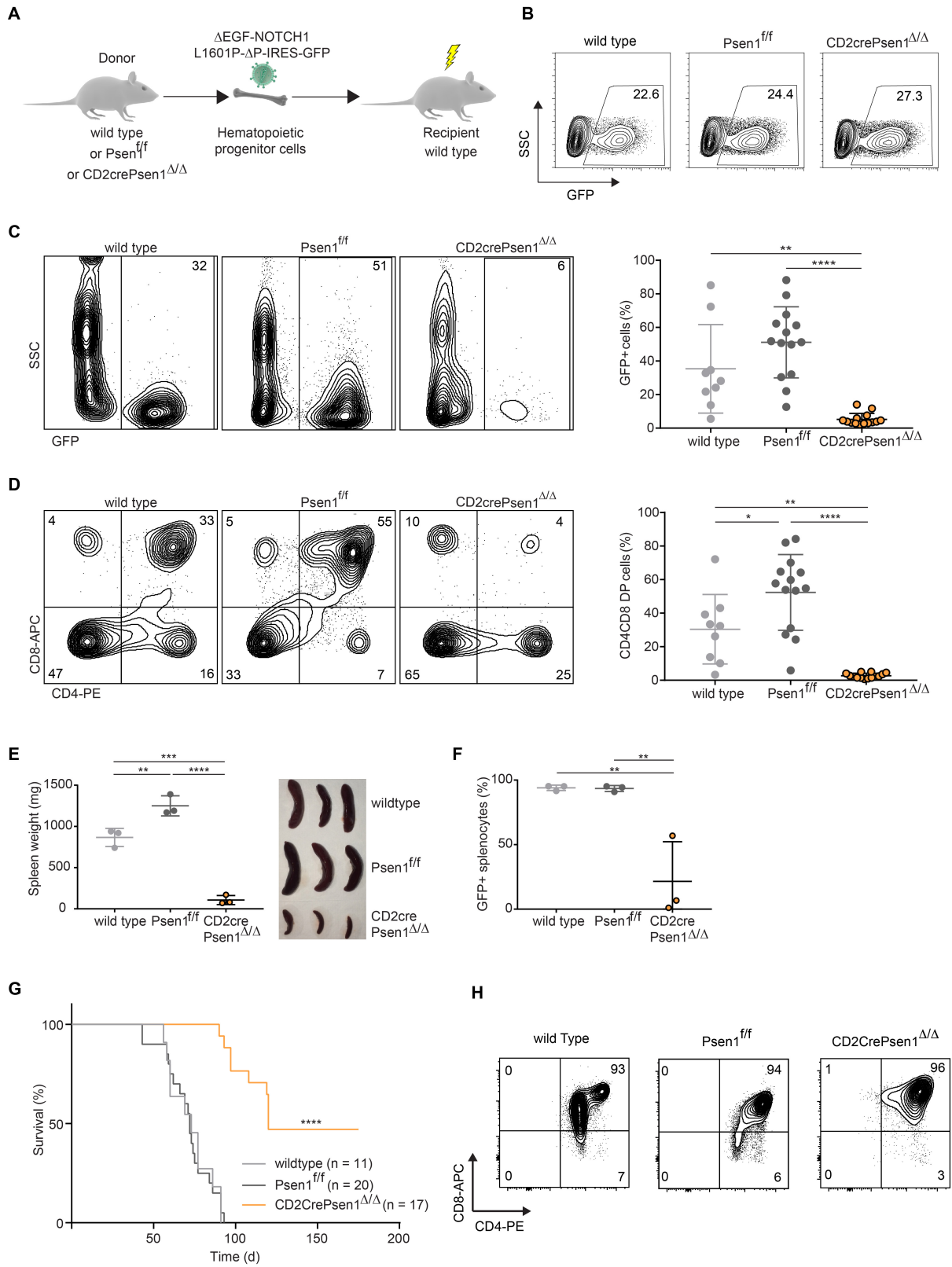


Fig. 2. PSEN1 deletion impairs mutant NOTCH1-induced T-ALL development.

(A) Schematic of primary bone marrow transplant using hematopoietic stem and progenitor cells from C57BL/6 *wild type*, *Psen1^{ff}*, or *CD2CrePsen1^{Δ/Δ}* donor mice transduced with MSCV-ΔEGF-NOTCH1-L1601P-ΔP-IRES-GFP transplanted into sublethally irradiated wild type C57BL/6 recipient mice. (B) Representative flow cytometry plots for the numbers of GFP⁺ transduced lineage-negative cells before injection into recipient mice. (C) Representative flow cytometry plots for the numbers of circulating GFP⁺ cells in peripheral blood from mice transplanted with *wild type*, *Psen1^{ff}*, or *CD2CrePsen1^{Δ/Δ}* progenitors expressing ΔEGF-NOTCH1-L1601P-ΔP 6 weeks after transplantation. Quantification of the GFP⁺ population is shown on the right (n=9, 14, and 14 mice, respectively). (D) Representative flow cytometry plots of peripheral blood from mice transplanted with *wild type*, *Psen1^{ff}*, or *CD2CrePsen1^{Δ/Δ}* progenitors expressing ΔEGF-NOTCH1-L1601P-ΔP stained with antibodies to CD4 and CD8 6 weeks after transplantation. Quantification of the CD4⁺CD8⁺ double-positive (DP) population is shown on the right (n=9, 14, and 14 mice, respectively). (E) Size and weight of spleens from mice transplanted with *wild type*, *Psen1^{ff}*, or *CD2CrePsen1^{Δ/Δ}* progenitors expressing ΔEGF-NOTCH1-L1601P-ΔP analyzed 9 weeks after transplantation (n=3). (F) Quantification of GFP⁺ cells in spleens from mice transplanted with *wild type*, *Psen1^{ff}*, or *CD2CrePsen1^{Δ/Δ}* progenitors expressing ΔEGF-NOTCH1-L1601P-ΔP analyzed 9 weeks after transplantation (n=3). (G) Kaplan-Meier survival curves of mice transplanted with *wild type*, *Psen1^{ff}*, or *CD2CrePsen1^{Δ/Δ}* progenitors expressing ΔEGF-NOTCH1-L1601P-ΔP. All graphs show the mean values, and error bars represent standard deviation. (H) Representative flow cytometry of end-stage leukemia in the different cohorts of mice. P-values in C, D, E, and F were calculated using one-way ANOVA. * P ≤ 0.05, ** P ≤ 0.01, *** P ≤ 0.001, and **** P ≤ 0.0001. P-value in F was calculated using the log-rank test. **** P ≤ 0.0001.

Fig. 3

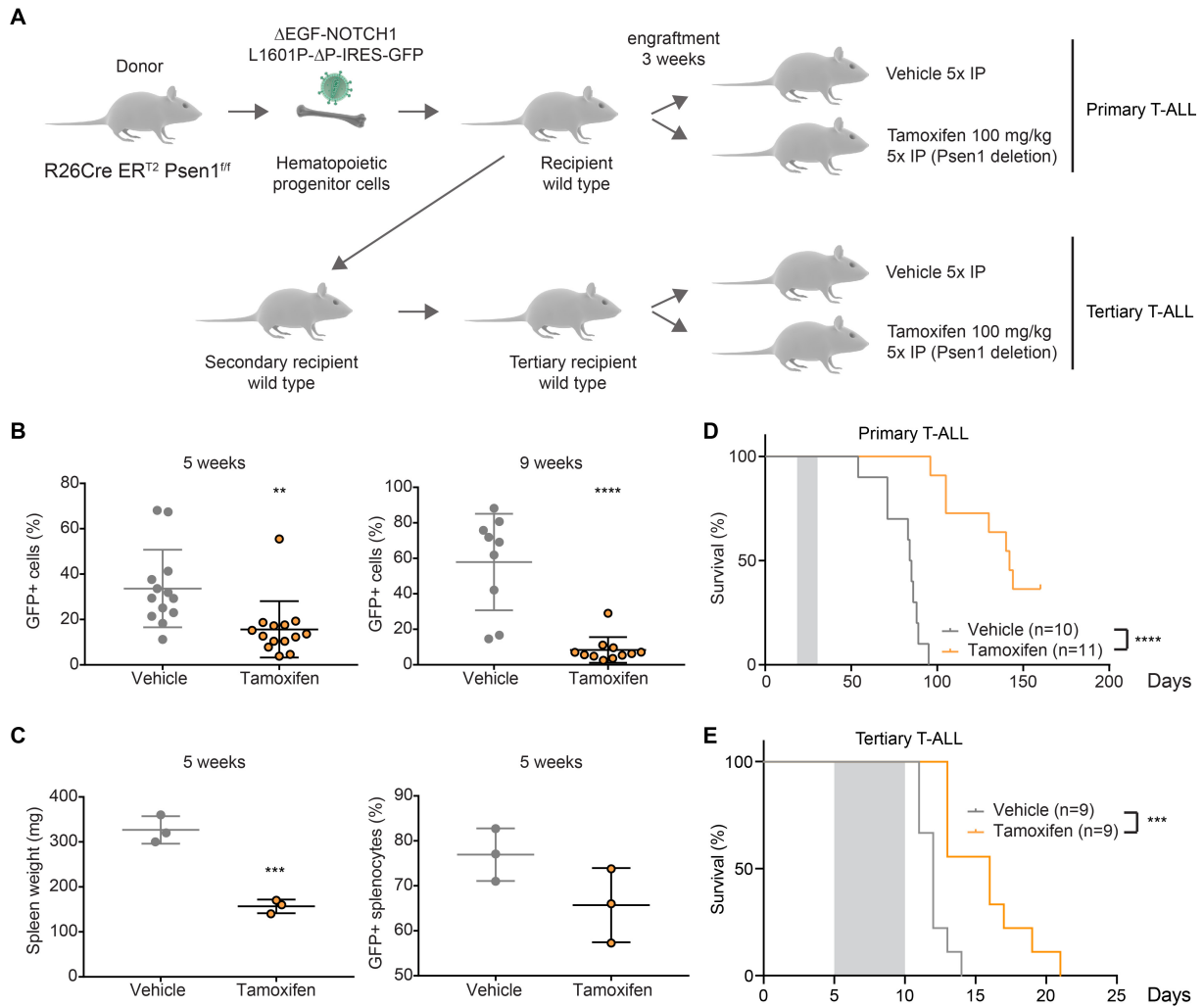


Fig. 3. Genetic targeting of PSEN1 impairs mutant NOTCH1 leukemia maintenance.

(A) Schematic of primary bone marrow transplant using hematopoietic stem and progenitor cells from *R26Cre-ER^{T2}Psen1^{ff}* donor mice transduced with MSCV- Δ EGF-NOTCH1-L1601P- Δ P-IRES-GFP before transplantation into sublethally irradiated wild type C57BL/6 recipient mice. Once engraftment was confirmed (3 weeks after transplantation), primary transplant mice were either treated with 100 mg/kg/day tamoxifen (or vehicle) by IP injection on 5 consecutive days to delete PSEN1 specifically in transplanted donor cells or used for secondary/tertiary transplants before treatment with 100 mg/kg/day tamoxifen by IP injection on 5 consecutive days to delete PSEN1. (B) The numbers of circulating GFP⁺ cells in peripheral blood from mice transplanted with *R26Cre-ER^{T2}Psen1^{ff}* progenitors expressing Δ EGF-NOTCH1-L1601P- Δ P after tamoxifen or vehicle treatment 5 weeks (n=13 and n=14 mice, respectively) and 9 weeks after transplant (n=9 and n=11 mice, respectively). (C) Spleen weight and quantification of GFP⁺ cells in spleens from mice transplanted with *R26Cre-ER^{T2}Psen1^{ff}* progenitors expressing Δ EGF-NOTCH1-L1601P- Δ P 5 weeks after transplant, treated with either vehicle or

tamoxifen (n=3 mice). **(D)** Kaplan-Meier survival curves of primary *R26Cre-ER^{T2}Psen1^{fl/fl}* transplant mice expressing Δ EGF-NOTCH1-L1601P- Δ P treated with either vehicle or tamoxifen. **(E)** Kaplan-Meier survival curves of tertiary *R26Cre-ER^{T2}Psen1^{fl/fl}* mice expressing Δ EGF-NOTCH1-L1601P- Δ P treated with either vehicle or tamoxifen. Gray boxes represent the treatment period. All graphs show the mean values, and error bars represent standard deviation. P-values in **B** and **C** were calculated using two-tailed Student's t-test. ** $P \leq 0.01$, *** $P \leq 0.001$, and **** $P \leq 0.0001$. The P-value in **D** was calculated using the log-rank test. **** $P \leq 0.0001$. (Vehicle = corn oil)

Fig. 4

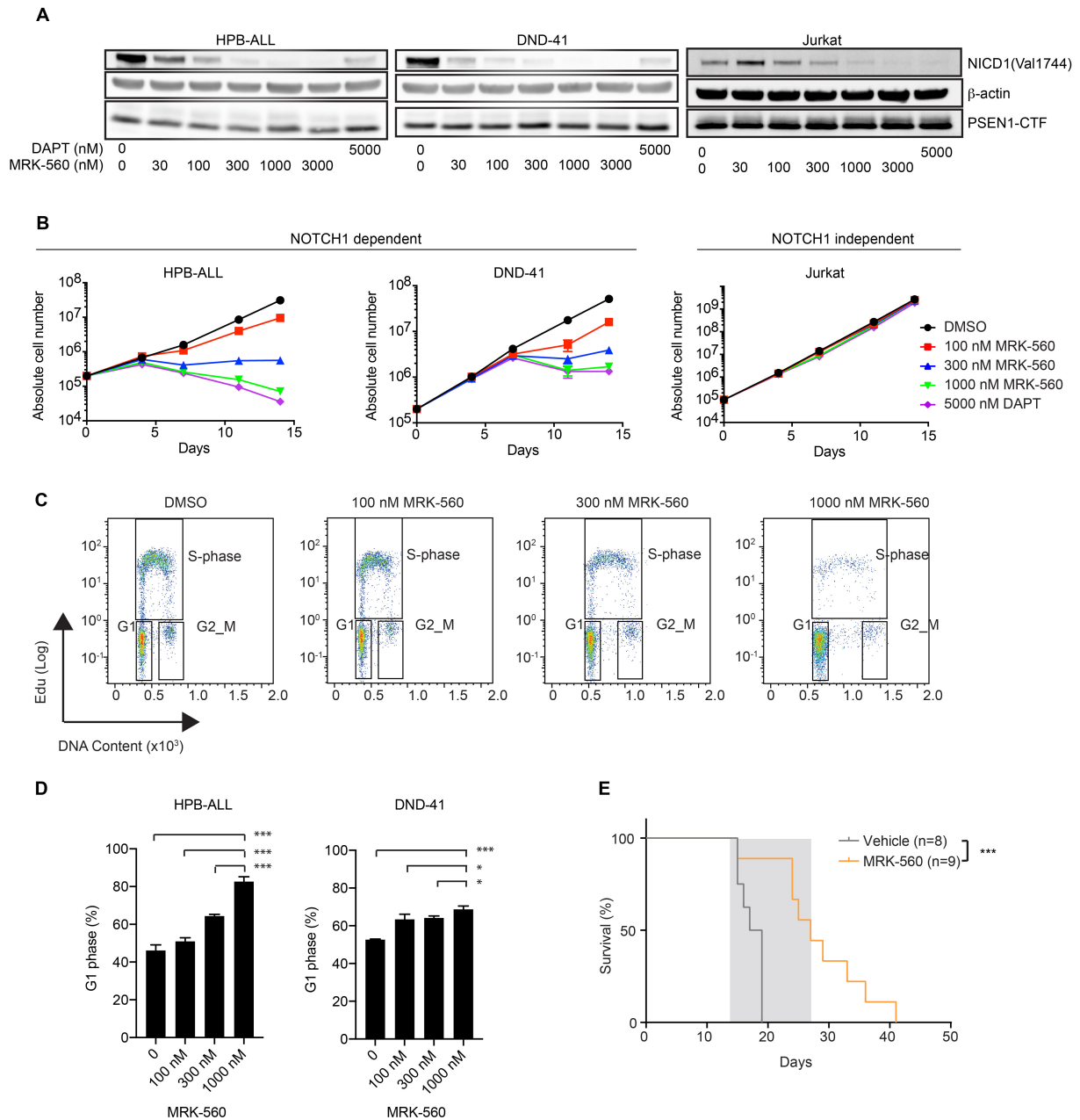


Fig. 4. PSEN1 selective inhibition impairs T-ALL cell proliferation.

(A) Western blot analysis for NICD1 in HPB-ALL, DND-41, and Jurkat cells in response to MRK-560 and DAPT treatment. (B) Proliferation of NOTCH-dependent HPB-ALL and DND-41 cells and NOTCH-independent Jurkat cells in response to MRK-560 (n=3). (C) Cell cycle analysis of HPB-ALL cells treated with increasing doses of MRK-560. (D) Quantification of the percentages of HPB-ALL and DND-41 cells in G1 phase upon treatment with increasing doses of MRK-560. (E) Kaplan-Meier survival curves for mice with Δ EGF-NOTCH1-L1601P- Δ P-induced leukemia treated with vehicle or 30 μ mol/kg/day MRK-560 for 14 days. Gray boxes represent the treatment period. Graphs show the

mean values, and error bars represent standard deviation. P-values in **B** were calculated using two-way ANOVA, P-values in **C** were calculated using the log-rank test, * $P \leq 0.05$, ** $P \leq 0.01$, and **** $P \leq 0.0001$. (DMSO: Dimethyl sulfoxide; DAPT: N-[N-(3,5-Difluorophenacetyl)-L-alanyl]-S-phenylglycine t-butyl ester)

Fig. 5

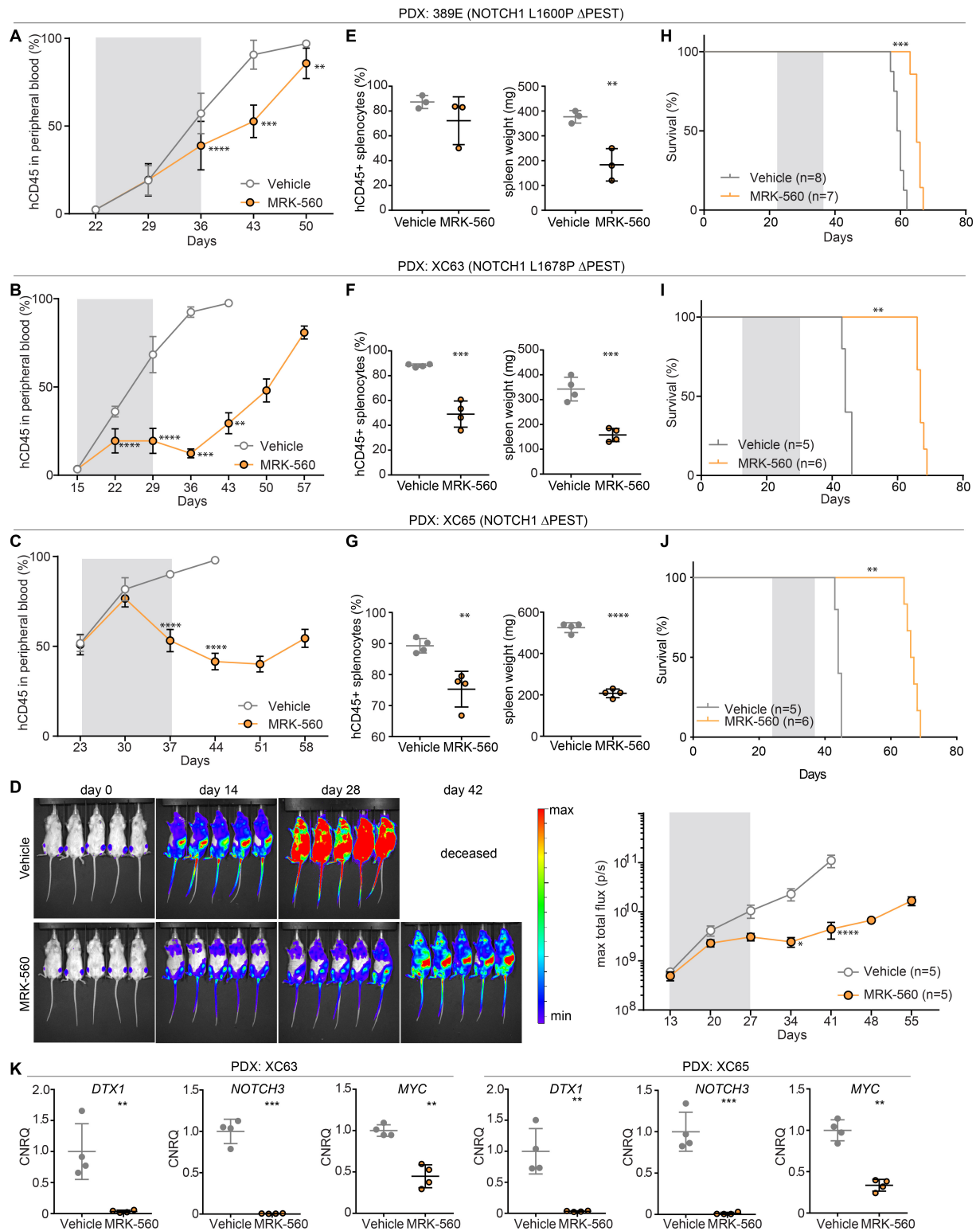


Fig. 5. Pharmacological PSEN1 inhibition attenuates leukemia in patient-derived xenografts. Percentages of human CD45⁺ cells in peripheral blood from mice transplanted with patient samples (A)

389E, **(B)** XC63, and **(C)** XC65 treated with vehicle or 30 $\mu\text{mol/kg/day}$ MRK-560 for 14 days. **(D)** Bioluminescence images depicting mice with leukemia burden closest to the mean among animals transplanted with patient sample XC65 and treated with vehicle or MRK-560 for 14 days. Quantification is shown in the right panel. **(E,F,G)** Quantification of human CD45⁺ cells in spleen and overall spleen weight from mice transplanted with patient samples **(E)** 389E, **(F)** XC63, and **(G)** XC65 after 14 days of treatment with vehicle or MRK-560 (n=3 for 389E and n=4 for XC63 and XC65). **(H,I,J)** Kaplan-Meier survival curves of mice transplanted with patient samples **(H)** 389E, **(I)** XC63, and **(J)** XC65 and treated with vehicle or MRK-560 for 14 days. Treatment of XC65 with MRK-560 and survival analysis began once leukemia burden was shown to be high in the blood (~50% hCD45⁺ cells). **(K)** qPCR analysis of *DTXI*, *NOTCH3*, and *MYC* expression in splenocytes from mice transplanted with patient sample XC63 or XC65 after 14 days of vehicle or MRK-560 treatment (n=4). Graphs show the mean values, and error bars represent standard deviation. Gray boxes represent the treatment period. P-values in **A**, **B**, **C**, and **D** were calculated using two-way ANOVA and two-tailed Student's t-test, P-values in **E**, **F**, **G**, and **K** were calculated using two-tailed Student's t-test, and P-values in **H**, **I**, and **J** were calculated using the log-rank test, ** $P \leq 0.01$, *** $P \leq 0.001$, and **** $P \leq 0.0001$. (Vehicle: 20% hydroxypropyl- β -cyclodextrin (HP β CD) in 0.1 M meglumine)

Fig. 6

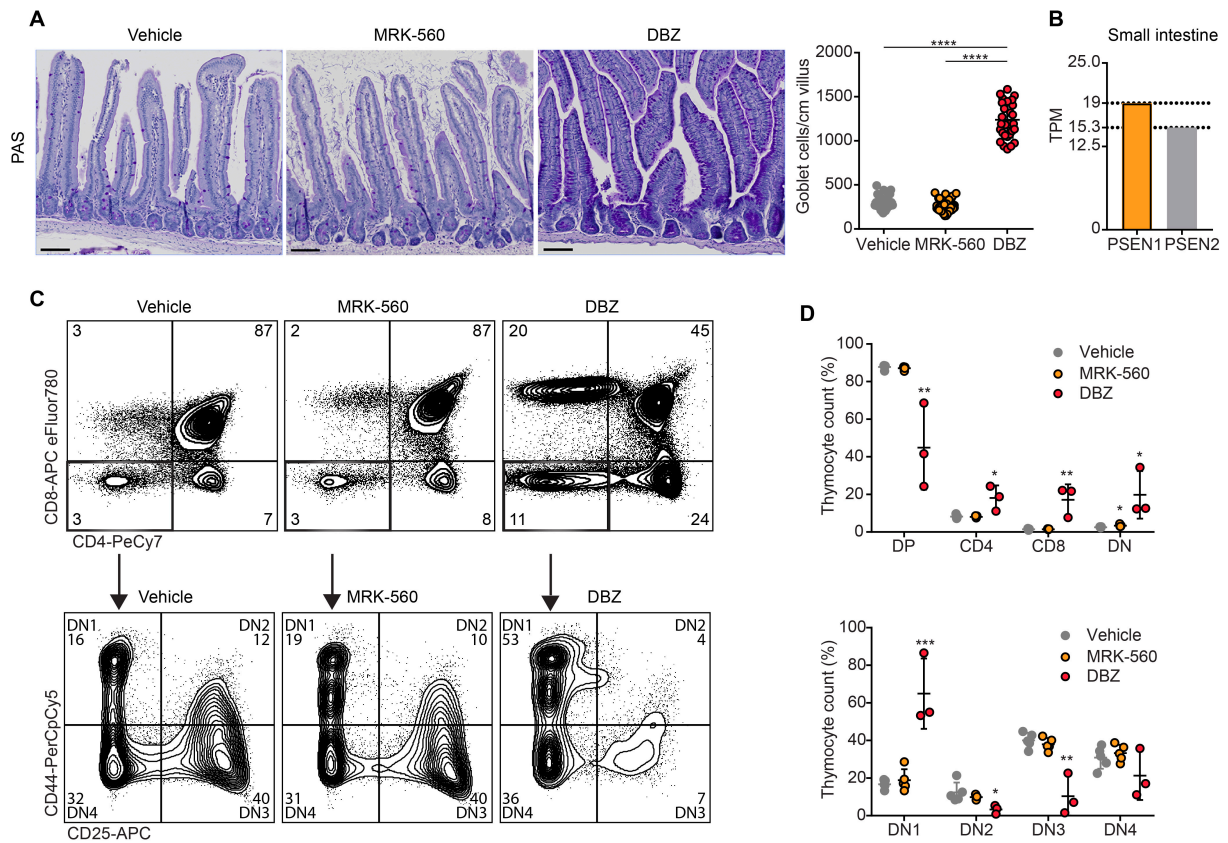


Fig. 6. Pharmacological selective PSEN1 targeting does not cause gastrointestinal toxicity or T cell developmental defects.

(A) Representative images of periodic acid-Schiff staining of intestines from mice treated with vehicle, MRK-560, or the broad-spectrum γ -secretase inhibitor dibenzazepine (DBZ) for 14 days to assess the number of secretory goblet cells. Scale bars represent 100 μ m. Quantification of the number of goblet cells per cm of villus is shown on the right (vehicle n=4, MRK-560 n=4, and DBZ n=3). (B) Human *PSEN1* and *PSEN2* gene expression in small intestine. Data for this analysis were obtained from the GTEx portal and dbGaP accession number phs000424.vN.pN. (C) Representative flow cytometry plots of thymocyte populations stained with antibodies to CD4 and CD8 or CD44 and CD25 in C57BL/6 mice treated with vehicle, MRK-560, or DBZ for 14 days. (D) Quantification of intrathymic T cell populations in relative numbers (vehicle n=5, MRK-560 n=5, and DBZ n=3). All graphs show the mean values, and error bars represent standard deviation. The P-values in A and D were calculated using one-way ANOVA. * $P \leq 0.05$, ** $P \leq 0.01$, *** $P \leq 0.001$, and **** $P \leq 0.0001$.